ELSEVIER

Coordination Chemistry Reviews 230 (2002) 263–282

COORDINATION CHEMISTRY REVIEWS

www.elsevier.com/locate/ccr

To be or not to be NO in coordination chemistry? A mechanistic approach

Maria Wolak [a,b], Rudi van Eldik [a,*]

[a] *Institute for Inorganic Chemistry, University of Erlangen-Nürnberg, Egerlandstrasse 1, 91058 Erlangen, Germany*
[b] *Faculty of Chemistry, Jagiellonian University, 30060 Krakow, Poland*

Received 14 September 2001; accepted 14 December 2001

Contents

Abstract . . . 263
1. Introduction . . . 263
2. Structure and electronic properties of metal nitrosyls . . . 264
   2.1. Nitrosylmetalloporphyrins . . . 264
   2.2. Ferrous chelate nitrosyls . . . 266
3. Interaction of NO with model Fe^{II}(L) complexes . . . 267
4. Interaction of NO with biomolecules . . . 270
   4.1. Myoglobin, haemoglobin and metmyoglobin . . . 270
   4.2. Cytochrome c^{II} and c^{III} . . . 273
   4.3. Reduced vitamin B_{12} . . . 274
5. Problems in the study of reactions of NO with metal complexes in solution . . . 277
   5.1. Is the reactive species NO or NO_2^-/HONO? . . . 277
   5.2. Interactions of nitrite with transition metal complexes . . . 278
6. Conclusions . . . 281
Acknowledgements . . . 281
References . . . 281

Abstract

In this review, the reactions of nitric oxide with selected metal complexes of biological and environmental importance are reviewed. Fundamental chemical kinetics and mechanisms that lead to the formation and decay of nitrosyl complexes are illustrated and discussed on the basis of work on Fe(II) chelate complexes and selected biomolecules such as metmyoglobin and cobalamin. In the context of common interference of higher nitrogen oxides in the studies on the interactions of nitric oxide with metal centres, the reactions of NO_2^-/HONO (in aqueous media) and NO_2/N_2O_3 (in aprotic media) with metal complexes are described on the basis of selected examples. Throughout the review the focus is on the mechanistic details of the binding of NO to and the release of NO from metal complexes, and the nature of the stable metal–NO complexes produced in solution.

Keywords: Nitric oxide; Nitrosyl complexes; Mechanistic approach

1. Introduction

Reactions of nitric oxide (NO) with transition metal ions play an important role in environmental and biological processes. Much of their significance is related to the interaction of NO with iron porphyrins [1,2] and non-haem iron complexes [3,4]. The biological and environmental importance of such interactions has stimulated research on the kinetics and mechanisms of the binding and release of NO from these complexes, as well as on the characterisation of the reaction products.

* Corresponding author. Tel.: +49-9131-8527350; fax: +49-9131-8527387
E-mail address: vaneldik@chemie.uni-erlangen.de (R. van Eldik).

0010-8545/02/$ - see front matter
PII: S0010-8545(01)00472-6

These studies were aimed at a better understanding of the fundamental chemistry of metal–NO interactions under biological conditions. In this context, particular attention was given to the reactions between NO and haem and non-haem iron centres of metalloproteins. In addition, a large number of model complexes have been studied. These mainly include synthetic metalloporphyrins of the first row transition metals (especially Fe(II) and Fe(III)), and Fe(II) chelate complexes, which may serve as models for iron centres in non-haem metalloproteins [1–5]. The latter class of compounds has also received considerable attention as potential catalysts for the removal of NO from exhaust gas streams, which was aimed at finding inexpensive and highly soluble metal chelates for selective and efficient binding of NO in aqueous solution.

Kinetic and spectroscopic measurements revealed large differences in the reactivity of metal complexes towards NO, as well as in the nature of the resulting nitrosyl species [1,6]. This rich chemistry results, on the one hand, from the free radical character of NO, and on the other hand, from the influence of the metal and its ligand environment on reactivity towards NO. Despite the extensive studies on the metal–NO interactions, the fundamental chemistry of thermal processes by which NO forms and breaks bonds with the metal are still not well characterised. Nevertheless, numerous kinetic and spectroscopic measurements provide a general mechanistic picture for such interactions: while the radical nature of NO is important in determining the stability and chemical properties of the resulting metal nitrosyls, the reaction dynamics is dominated by the lability of the metal centre [1].

Over the past few years we have developed an interest in the mechanistic understanding of the interaction of NO with different metal complexes and metalloproteins. We have performed detailed mechanistic studies, including the application of various spectroscopic and high pressure kinetic techniques, on a variety of systems that are of environmental and biological significance. During this work we often ran into the question whether it is really NO that is the reactive molecule, and what the formal nature of NO is once it is bound to a metal centre. In that sense, we would here like to focus on the central question 'To be or not to be NO in coordination chemistry?', in terms of the reactive species in solution and the nature of the coordinated ligand. In the present review, reactions of nitric oxide with selected metal complexes of biological and environmental importance are surveyed. Fundamental chemical kinetics and mechanisms that lead to the formation of nitrosyl complexes are illustrated and discussed on the basis of our work on Fe(II) chelate complexes and selected biomolecules (such as metmyoglobin and vitamin B_{12}).

2. Structure and electronic properties of metal nitrosyls

Binding of NO to a metal centre must result in the stabilisation of NO, a radical species in the ground state. Such stabilisation can be achieved by a shift of electron density to the metal centre or to the nitrosyl ligand, and can formally be described as the formation of the nitrosyl cation (NO^+) or the nitroxyl anion (NO^-), respectively, as depicted by the mesomeric structures in reactions (1a) and (1b).

$$(L)M^{n+} + NO \rightleftharpoons (L)M^{n+}\text{–}NO \leftrightarrow (L)M^{(n-1)+} - NO^+ \quad \text{linear M–N–O group} \tag{1a}$$

$$(L)M^{n+} + NO \rightleftharpoons (L)M^{n+}\text{–}NO \leftrightarrow (L)M^{(n+1)+}\text{–}NO^- \quad \text{bent M–N–O group} \tag{1b}$$

The initially proposed description of metal–nitrosyl complexes as derivatives of either NO^+ or NO^-, although in many cases useful in describing the two limiting geometries of the M–N–O group (linear or bent), did not allow a uniform description of their properties. A preferable description of metal nitrosyls was, however, offered by Enemark and Feltham in 1972 [7]. Their theory was based on an electron counting formalism and states that 'the structure and properties of nitrosyl complexes are best understood by considering the $\{M\text{–}NO\}^n$ group (where n represents the sum of the metal d and NO π^* electrons) as an 'inorganic functional group' perturbed by the field imposed by other ligands attached to the metal [7].' According to this description, the main focus of this review is on penta-, hexa- and hepta-coordinate nitrosyl complexes of iron and cobalt with the total number of electrons within the $\{M\text{–}NO\}$ unit $n = 6$, 7, and 8. The M–NO group in these complexes adopts a linear or bent configuration (depending on n and on ligand environment of metal), which can be often correlated with the formal oxidation or reduction of the nitrosyl ligand upon its coordination to the metal centre. Thus the coordination chemistry question remains: is it NO, NO^+ or NO^- when coordinated to a metal centre?

2.1. Nitrosylmetalloporphyrins

Numerous metalloporphyrins react with NO to give stable adducts. Due to the significant biological importance of these interactions, a substantial amount of literature on the topic has already been published, and the currently available information on synthesis, structure and properties of nitrosyl metalloporphyrins has been summarised elsewhere [1,2]. For this reason we present here only the most important features of metalloporphyrin nitrosyls, which may be helpful in the discussion of kinetic and mechanistic aspects of metalloporphyrin–NO interactions presented later.

An important feature of porphyrin-based complexes is the presence of the porphyrin equatorial ligand which induces a square-pyramidal or a pseudo-octahedral geometry of the nitrosyl complexes (for the five- and six-coordinate species, respectively), i.e. molecules with a nearly C_{4v} symmetry. Coordination of NO to the parent metalloporphyrins induces a low spin electronic configuration of the metal centre in the resulting nitrosyl derivatives [1]. Application of the Enemark and Feltham formalism to such low-spin metal nitrosyls with nearly C_{4v} symmetry predicts a linear geometry of the M–NO group for all the structures with $n = 6$, whereas for $n \geq 7$ a bent M–NO unit is anticipated [7]. These predictions are in agreement with experimental observations which clearly show a systematic variation in the M–N–O angle and M–NO bond length along the $\{M–NO\}^n$ series with increasing n [2]. This can be illustrated by a series of synthetic Fe^{III}(P)NO, Fe^{II}(P)NO and Co^{III}(P)NO complexes (where P denotes a porphyrinate ligand), in which the differences in M–N–O angles and M–NO bond lengths indicate the gradual changeover from a linear $M–NO^+$ unit (observed for the Fe^{III}(P)NO complex with $n = 6$) to a strongly bent $M–NO^-$ group (observed for the Co^{II}(P)NO species with $n = 8$) [1,2]. These changes are accompanied by variation within the geometry of the square-pyramidal $M(N_{eq})NO$ coordination group, as shown in schematic diagrams for M(P)NO complexes with $n = 6$, 7 and 8 (Fig. 1) [2]. In addition, close examination of crystal structures of iron(II) porphyrin nitrosyls revealed small but characteristic off-axis tilt of the Fe–NO bond vector and the apparently correlated asymmetry pattern in the equatorial $Fe–N_{eq}$ bond distances (see Fig. 1b) [2]. The distortions observed have been reported as an intrinsic structural feature of all $\{Fe–NO\}^7$ porphyrin nitrosyls [2,8] and rationalised in terms of the specific molecular orbital interactions present in this class of compounds [8–10]. It is, however, worth noting that structural and electronic features typical for $\{Fe–NO\}^7$ porphyrinates can also be observed in nitrosyl porphyrins which are formally $\{M–NO\}^6$ species, as shown by a recent study on nitrosylated organometallic porphyrinate complexes of Fe(III) and Ru(III), viz. Fe(OEP)(NO)(p-C_6H_4F) and Ru(OEP)(NO)(p-C_6H_4F) [10]. Bending and tilting of the MNO group observed in these complexes apparently result from the presence of the strong σ-donating aryl ligand, which imposes a high electron density on the Fe(III) (or Ru(III)) centre and thus induces specific electronic interactions typical for that observed in iron(II) porphyrin nitrosyls.

An important feature of the nitrosylmetalloporphyrins is a *trans*-labilisation effect of the coordinated NO ligand observed in the $\{M–NO\}^7$ and $\{M–NO\}^8$ systems. While the $\{M–NO\}^6$ species are usually six-coordinate complexes, the affinity of the basically five-coordinate $\{M–NO\}^7$ nitrosyls for a sixth ligand is quite small, and even further reduced in the case of the $\{M–NO\}^8$ systems [2].

A variety of spectroscopic techniques can be used to study nitrosyl derivatives of metalloporphyrins. Due to the usual low-spin electronic configuration of the metal centre in nitrosylated metalloporphyrins, the $\{M–NO\}^6$ and $\{M–NO\}^8$ porphyrin nitrosyls are typically diamagnetic, while those of $\{Fe–NO\}^7$ exhibit a paramagnetic ground spin state of $S = 1/2$. Application of EPR spectroscopy to the latter class of compounds yields useful information on their electronic and geometrical structure [1,2,11]. On the other hand, diamagnetic $\{M–NO\}^6$ and $\{M–NO\}^8$ nitrosyls can be effectively studied by ^{15}N-NMR spectroscopy, which provides a direct indication of the electron density on the coordinated NO ligand [12–14].

Infrared spectroscopy has often been used in the assignment of the charge distribution in the M–N–O group. Despite the well-known interpretation problems associated with this technique, the nitrosyl stretching frequencies were used as a probe for the NO^+ or NO^- character of the coordinated NO ligand in iron porphyrin nitrosyls [2]. New insight into the electronic

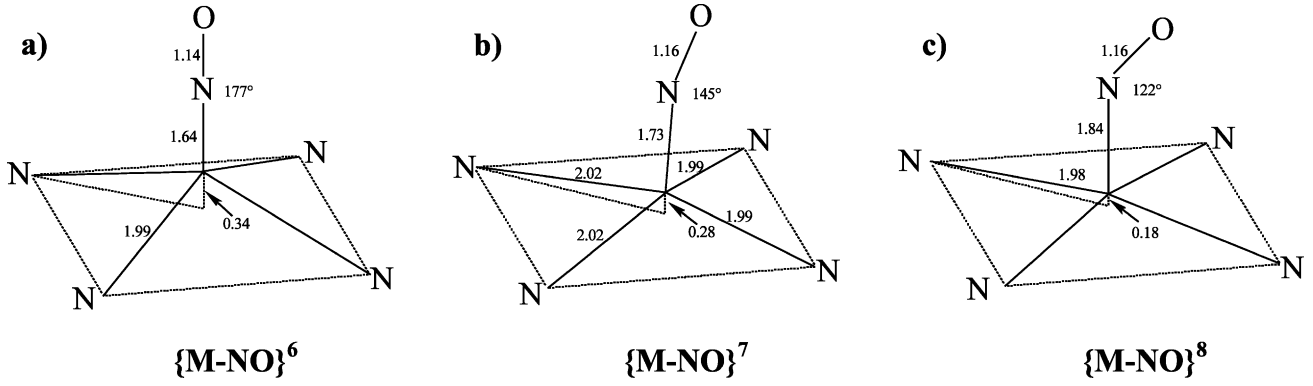

Fig. 1. 'Consensus' structures based on available structural data on the $M(N_{eq})NO$ coordination group in nitrosylporphyrin series $\{M–NO\}^n$ with $n = 6$, 7 and 8.

configuration of the $\{Fe–NO\}^n$ group comes from Mössbauer spectroscopic studies, which are capable of providing information on the electronic configuration of the iron centre [10,15]. Interpretation of the results obtained with this experimental method is, however, not straightforward and should be based on analyses of data obtained for a series of structurally similar complexes [10,16]. Furthermore, comparison of results obtained with IR techniques with those obtained from Mössbauer spectroscopic studies, shows that these two indicators of charge distribution in the $\{Fe–NO\}^n$ unit can be inconsistent [15]. This complication presumably arises form a highly covalent nature of the $\{Fe–NO\}^n$ unit in which the spin density is delocalised over the entire M–NO group [2,8,15]. Although the assignment of the electronic configuration for porphyrinate $\{Fe–NO\}^n$ units with the aid of Mössbauer spectroscopy is preferable to a formal assignment of the NO oxidation state, this description is not always satisfactory when all the experimental data are considered [15].

The electronic absorption spectra of metalloporphyrins are dominated by strong $\pi–\pi^*$ intraligand transitions, which are, however, affected by the nature of the metal and the axial ligands coordinated to the metal centre [1,2]. Thus, examination of the UV–Vis spectra of porphinato metal nitrosyls often yields information on the electronic and geometrical structure of a given nitrosyl complex [2]. In addition, UV–Vis spectroscopy is widely used in kinetic studies on the interaction of metalloporphyrins with NO.

2.2. Ferrous chelate nitrosyls

Nitric oxide reversibly binds to numerous iron(II) chelates. The resulting nitrosyl complexes, which according to the Enemark and Feltham formalism represent $\{Fe–NO\}^7$ species, differ to some extend from porphyrinate $\{M–NO\}^7$ adducts. This mainly results from the difference in ligand environment of the iron centre, which in this case is not restricted by the equatorial porphyrin ligand. A variety of chelate ligands which can coordinate to the iron(II) centre create ligand fields of different strength and symmetry. These differences are apparently reflected in the properties of the nitrosyl derivatives obtained from the parent iron(II) chelates.

Extensive research on chelate $\{Fe–NO\}^7$ nitrosyls has been initiated by the observation of an unusual $S = 3/2$ ground spin state in nitrosylated non-haem iron proteins, which results from the addition of the odd electron of NO ($S = 1/2$) to a high spin ($S = 2$) Fe(II) site [3,4,17,18]. This led to the application of nitric oxide as a useful paramagnetic probe for dioxygen binding in studies on dioxygen activation by non-haem iron proteins. Many examples of quartet spin state $\{Fe–NO\}^7$ species can be found within a series of Fe(II) complexes with aminocarboxylate and pyridylmethylamine ligands [4,19,20]; for instance, the well-known seven-coordinate $[Fe(edta)NO]^{2-}$ complex exhibits this spin behaviour [17].

Nitrosyl complexes of iron(II) have been characterised as six- and seven-coordinate species with a quartet ($S = 3/2$) [3,4,19,20] or doublet ($S = 1/2$) [16,20–22] ground spin state. The $\{Fe–NO\}^7$ class of compounds with the net spin state $S = 3/2$, presents an interesting case in which the metal–NO interactions within the $\{M–NO\}^n$ group cannot be described by the MO treatment proposed by Enemark and Feltham [7]. Such description is, however, offered by the spin-polarisation model. According to this model, the electronic structure of a $\{Fe–NO\}^7$ unit with the net spin state $S = 3/2$ can be described as a high-spin Fe(III) centre ($S = 5/2$) antiferromagnetically coupled to two unpaired electrons on NO^- ($S = 1$). Thus, the formal oxidation states within a $\{Fe–NO\}^7$ unit can be assigned as $\{Fe^{3+}–NO^-\}$ [16,17,19,20]. Such description is based on consistent results provided by EXAFS and XAS Fe-edge measurements, resonance Raman, magnetic circular dichroism and EPR spectroscopy, magnetic susceptibility measurements and advanced theoretical calculations [17]. These results were confirmed recently by applied-field Mössbauer spectroscopic investigations on a complete series of isostructural complexes containing $\{Fe–NO\}^{6/7/8}$ motives [16].

Ferrous chelate nitrosyls of the type $\{Fe–NO\}^7$ ($S = 1/2$), i.e. possessing the same ground spin state as that observed for porphyrin $\{Fe–NO\}^7$ species, and a few cases of spin-crossover systems which show the equilibrium $S = 3/2 \leftrightarrow S = 1/2$ have also been reported in the literature [16,20,21]. In order to evaluate the influence of metal ligation on the net spin state of the chelate $\{Fe–NO\}^7$ nitrosyls, a series of $Fe^{II}(L)$ complexes with aminocarboxylate and pyridylmethylamine ligands of different ligand field strength were studied [19,20]. Results of these studies indicate that the electronic configuration of the $\{Fe–NO\}^7$ unit is tuned by the ligand environment of the metal centre. Whereas weak and moderate ligand fields promote formation of $\{Fe–NO\}^7$ ($S = 3/2$) nitrosyls, the $S = 1/2$ electronic isomers are formed in the presence of stronger ligand fields.

Practical applications of $Fe^{II}(L)$ complexes with respect to nitric oxide chemistry are based on their ability to effectively bind NO. However, although many iron(II) aminocarboxylate and pyridyl-based complexes form stable nitrosyl derivatives, they are also reactive towards dioxygen. This fact considerably limits their application in both industrial and biomedical applications [21,23]. Solving this and related problems requires a good knowledge of the fundamental chemistry involved in the interactions between $Fe^{II}(L)$ complexes and NO. Although extensive studies on structural and

electronic properties of iron(II) nitrosyls are helpful in this respect, mechanistic information on the interactions between NO and $Fe^{II}(L)$ complexes is apparently lacking. In this context, some important developments in mechanistic studies on such interactions, based on studies performed in our laboratories, are presented later in this review.

3. Interaction of NO with model $Fe^{II}(L)$ complexes

As pointed out in the previous section, chelate iron(II) nitrosyls belonging to the $\{Fe–NO\}^7$ class of complexes, differ in their structural and electronic features from the corresponding metalloporphyrin systems. An important question is to what extend these differences are reflected in the kinetics and mechanisms of their interactions with NO. This question, although interesting on its own, is of significant importance to biomedical and industrial applications of such Fe(II) chelates.

In contrast to the large body of kinetic and mechanistic data on the nitrosylation of iron porphyrin centres, little is known on the binding and release of NO from chelate Fe(II) complexes. As a consequence, the main factors that influence the thermodynamics and kinetics of these reactions are largely unknown. It is reasonable to expect, however, that such data could enable kinetic and thermodynamic control over NO binding to $Fe^{II}(L)$ complexes, and thus tuning of the overall process with respect to potential practical applications. Recent developments in this area include studies on aminocarboxylate iron(II) complexes with different chelating ligands derived from edta [23–25]. In these studies, a systematic variation of donor type and strength within a series of 38 selected ligands was undertaken in order to optimise the efficiency and reversibility of the binding of NO to the $Fe^{II}(L)$ complexes.

Nitrosation of an iron(II) chelate is expressed by reaction (2).

$$Fe^{II}(L)H_2O + NO \underset{k_{off}}{\overset{k_{on}}{\rightleftarrows}} Fe^{II}(L)NO + H_2O \quad (2)$$

This reaction describes the binding of NO to various chelate complexes with coordination number six or seven, in which a water molecule occupies one of the coordination sites. The presence of such a water molecule was detected in the crystal structure of the seven-coordinate $[Fe^{II}(edta)H_2O]^{2-}$ complex [26]. In addition, water exchange studies on several $Fe^{II}(L)$ complexes, performed with the aid of ^{17}O-NMR line broadening techniques, indicate that at least some of the complexes studied possess one or more coordinated water molecules [25]. It may be expected on the basis of information available on the reactions of other metal complexes with NO [1] that NO binding to such iron(II) chelates is probably not controlled by a simple addition process, but rather a substitution reaction of a labile water molecule by NO. However, as exact structural information on $Fe^{II}(L)$ complexes in solution is in many cases not yet available, coordinated water molecules will be omitted in the following formulae, unless their presence in a given complex is well established, and important for the discussion.

FTIR spectroscopic studies on the nature of nitrosylated aminocarboxylate complexes suggest a pronounced electron donation from the metal to NO. In the case of the $[Fe^{II}(edta)NO]^{2-}$ complex, a characteristic NO band is observed around 1777 cm^{-1} [23], and this complex has been shown to bind NO as $Fe^{III}–NO^-$ [17]. The slightly shifted bands for the other $[Fe^{II}(L)NO]^{x-}$ complexes also correspond to species formally written as $[Fe^{III}(L)(NO^-)]^{x-}$. However, the electronic structure of the $\{Fe–NO\}^7$ group in most of the $[Fe(L)NO]^{x-}$ complexes studied has not been determined in a more direct way.

A systematic study of the series of $Fe^{II}(L)$ complexes with different aminocarboxylate ligands indicated that their ability to reversibly bind NO is influenced strongly by the selected chelating ligand. This influence is apparent from the large variation in the overall binding constants, K_{NO} ($=k_{on}/k_{off}$), which span a wide range from ca. 1×10^3 to 2×10^7 M^{-1} for the complexes studied [23,24]. In addition, an interesting correlation was found between the stability of the $Fe^{III}(L)(NO^-)$ complexes and the oxygen sensitivity of the parent $Fe^{II}(L)$ complexes, i.e. their tendency to form $Fe^{III}(L)(O_2^-)$ species. From the comparison presented in Fig. 2, it can, in general, be concluded that the higher the K_{NO} value for a given metal nitrosyl, the larger the oxygen sensitivity of the parent $Fe^{II}(L)$ complex. Clearly, an increasing inductive effect of the chelate ligand causes an increase in stability of the $Fe^{III}–NO^-$ bond, and also enhances the shift of electron density from iron to oxygen in the corresponding $Fe^{III}(L)(O_2^-)$ complex.

A quantitative basis for the observed trends in the stability of the $Fe^{III}(L)(NO^-)$ complexes was provided by kinetic and mechanistic studies on the binding and release of NO from selected $Fe^{II}(L)$ complexes. The complexes exhibited quite different behaviour with respect to their reactions with NO. The observed differences are particularly large in the case of the Fe^{II}(mida) and Fe^{II}(edta) complexes: the mida complex shows almost no oxygen sensitivity, exhibits a low binding affinity for NO, and releases NO almost completely on passing an inert gas through the solution. In contrast, the edta complex is extremely oxygen sensitive, shows a very high binding affinity for NO and releases NO only slowly when treated with an inert gas.

Selected results from kinetic studies [24,27] performed with the complementary use of stopped-flow,

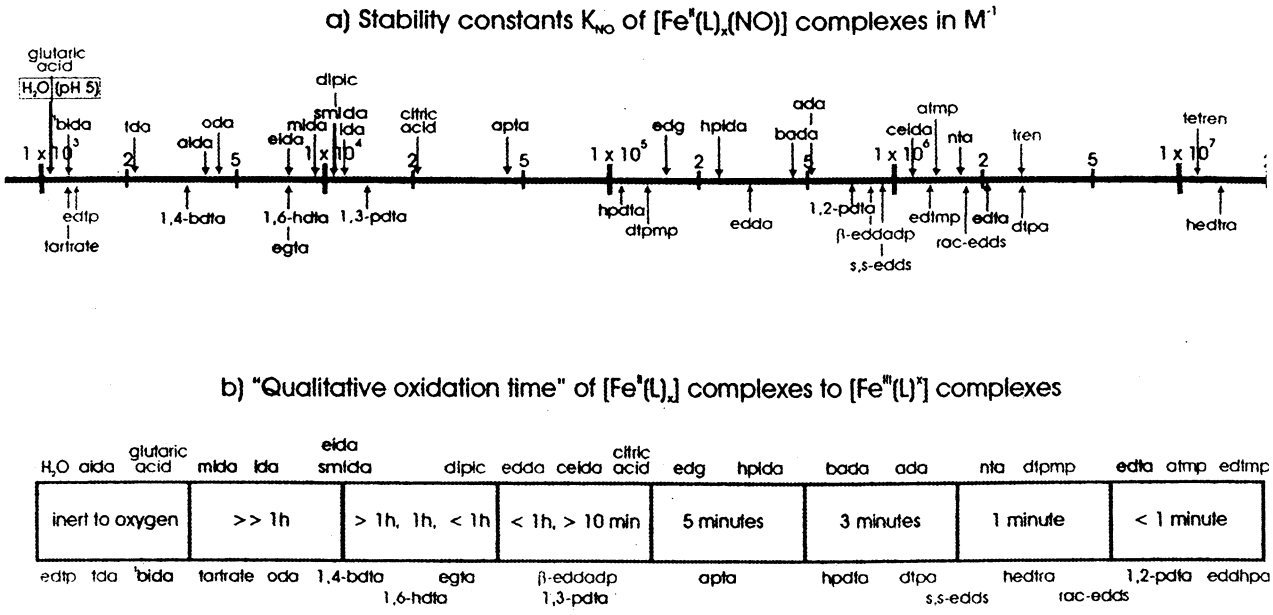

Fig. 2. Correlation between K_{NO} and qualitative oxidation time of $Fe^{II}(L)$ complexes (adapted from Ref. [23]).

Table 1
Summary of kinetic and thermodynamic parameters for the reversible binding of NO to a series of $Fe^{II}(L)$complexes

Complex	k_{on} [a] ($M^{-1}\,s^{-1}$)	k_{off} [a] (s^{-1})	$\Delta H^{\ddagger}$ (kJ mol^{-1})	$\Delta S^{\ddagger}$ (J $K^{-1}\,mol^{-1}$)	$\Delta V^{\ddagger}$ [a] ($cm^3\,mol^{-1}$)	K (k_{on}/k_{off}) [a] (M^{-1})	K [a,b] (M^{-1})
Fe^{II}(edta) (**1**)	2.4×10^8		24 ± 1	-4 ± 3	$+4.1 \pm 0.2$		
		91.0	61 ± 2	-5 ± 7	$+7.6 \pm 0.6$ [c]	2.1×10^6	2.1×10^6
Fe^{II}(hedtra) (**2**)	6.1×10^7		26 ± 1	-12 ± 3	$+2.8 \pm 0.1$		
		4.2	73 ± 1	11 ± 4	$+4.4 \pm 0.8$	1.1×10^7	1.5×10^7
Fe^{II}(mida) (**3**)	1.9×10^6		40 ± 1	8 ± 3	$+7.6 \pm 0.4$		
		57.3	47 ± 2	-55 ± 5	$+6.8 \pm 0.4$ [c]	2.1×10^4	9.5×10^3
$Fe^{II}(mida)_2$ (**4**)	1.8×10^6		34 ± 1	-13 ± 3	$+8.1 \pm 0.2$		
		62.2	64 ± 1	5 ± 5	$+5.1 \pm 0.5$ [c]	3.0×10^4	2.2×10^4
$Fe^{II}(H_2O)_6$ (**5**) [d]	1.6×10^6		37 ± 1	-3 ± 2	$+6.0 \pm 0.3$		
		3.2×10^3	48 ± 1	-15 ± 5	$+1.2 \pm 0.1$	5×10^2	1.2×10^3
Fe^{II}(nta) (**6**)	2.1×10^7		24 ± 1	-22 ± 3	-1.5 ± 0.1		
		9.3	66 ± 1	-5 ± 4	-3.5 ± 0.7	1.8×10^6	1.8×10^6

[a] Determined at 25 °C and at pH 5.0 unless otherwise stated.
[b] Determined thermodynamically from a combination of UV–Vis and potentiometric (NO electrode) techniques.
[c] Measured at 10 °C.
[d] Data from Ref. [27].

temperature jump, laser flash photolysis and pulse radiolysis techniques, are presented in Table 1. The thermodynamic and kinetic data obtained in the studies illustrate the fact that the overall binding constant, K_{NO}, for a given $Fe^{II}(L)$ complex is a net measure of its ability to bind and to release NO, and is therefore controlled by the forward and reverse rate constants. Thus, although the rate constant for the binding of NO to Fe^{II}(edta) is approximately four times larger than that observed for the Fe^{II}(hedtra) complex, the release of NO from Fe^{II}(edta)NO is approximately 22 faster than from Fe^{II}(hedtra)NO and this results in the lower stability constant observed for Fe^{II}(edta)NO. In another case, large differences in the K_{NO} values of Fe^{II}(edta) and Fe^{II}(mida) result from significantly different binding rate constants, k_{on}, obtained for these two complexes, whereas the k_{off} values are of the same order of magnitude. The Fe^{II}(nta) complex, which shows an intermediate behaviour in terms of its reversible binding of NO and oxygen sensitivity, has approximately the same stability constant, K_{NO}, as that observed for Fe^{II}(edta), but in this case both k_{on} and k_{off} are smaller. In the case of the aquated Fe(II) species, the binding of NO is as rapid as for the mida complexes, but the dissociation of NO is the fastest of all studied complexes and accounts for the unfavourable overall binding constant.

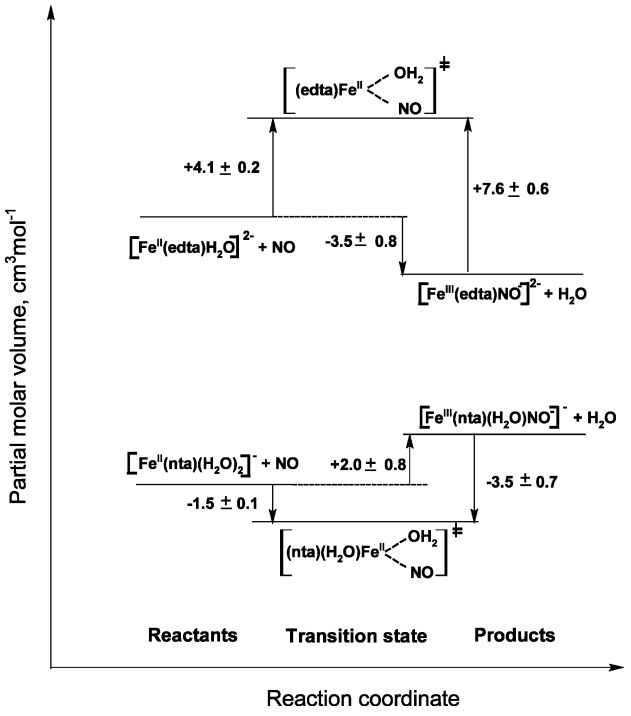

Fig. 3. Volume profiles for the reversible binding of NO to $[Fe^{II}(edta)H_2O]^{2-}$ and $[Fe^{II}(nta)(H_2O)_2]^{-}$.

More detailed insight into the mechanisms of the thermal reactions in which NO binds and dissociates from the iron centre in the $Fe^{II}(L)$ systems studied, comes from activation parameters for the 'on' and 'off' reactions obtained from systematic studies of k_{on} and k_{off} as a function of temperature and pressure (see Table 1) [25]. The positive volumes of activation found in most cases clearly indicate that the complex-formation reactions can be best described by a dissociative interchange (I_d) mechanism. The exception is the reaction of $Fe^{II}(nta)(H_2O)_2$ with NO, which exhibits a definite negative volume of activation, suggesting that the reaction occurs via an associative interchange (I_a) mechanism. The difference in the mechanism of nitrosylation observed for the $Fe^{II}(nta)(H_2O)_2$ complex as compared to the other studied complexes becomes clear from a comparison of the volume profiles for the edta and nta systems in Fig. 3. Such a variation in the mechanism presumably reflects the fact that $Fe^{II}(nta)(H_2O)_2$ is a six-coordinate complex [19,25], whereas it is known that $Fe^{II}(edta)H_2O$ is seven-coordinate [26]. This would mean that some complexes react according to an I_d mechanism as a result of their seven-coordinate, 20 valence electron character, whereas the six-coordinate nta complex reacts according to an I_a mechanism due to its 18 valence electron character. These results suggest that water exchange reactions on the studied $Fe^{II}(L)$ complexes presumably control the kinetics and mechanism of the NO binding.

Further support for this conclusion comes from a comparison of the activation parameters for the 'on' reactions obtained for $Fe(H_2O)_6^{2+}$, Fe(mida) and $Fe(mida)_2^{2-}$ with those resulting from water exchange studies performed on these systems [27,28] (see Table 2). The values of $\Delta H^{\ddagger}_{ex}$ and $\Delta V^{\ddagger}_{ex}$ for the water exchange process are similar to the corresponding activation parameters obtained for k_{on}, indicating that the binding of NO displays kinetic features similar to those observed for the water exchange reactions. This again suggests the displacement of coordinated water by NO as the rate-determining step, which is followed by a rapid intramolecular charge-redistribution process leading to the final product, $[Fe^{III}(L)(NO^{-})]$. The activation volumes obtained for the 'off' reactions (see Table 1 and Fig. 3) indicate that NO release from the $[Fe^{III}(L)(NO^{-})]$ complexes follows the similar interchange mechanism as that observed for the respective 'on' reaction. The rapid charge redistribution to form $[Fe^{II}(L)NO]$ prior to the rate-determining displacement of NO by water, can account for such an observation. Alternatively, the release of NO from $[Fe^{III}(L)(NO^{-})]$ can be visualised as a 'water assisted' homolysis reaction in which Fe^{III}–NO^{-} bond cleavage is accompanied by formal reduction of Fe(III) to Fe(II), and involves the simultaneous entry of a water molecule into the coordination sphere of Fe(II). The rate-determining step in the release of NO exhibits a much higher activation enthalpy than the 'on' reaction, which must be related to the strong Fe–NO bond and accounts for the significantly slower 'off' reactions.

It may be concluded that NO binding to the iron(II) chelate complexes studied is controlled by the lability of the iron centre in the parent $Fe^{II}(L)$ species, whereas the dissociation reaction is largely affected by the strength of the Fe–NO bond in the resulting $[Fe^{III}(L)(NO^{-})]$

Table 2
Kinetic parameters for water exchange reactions on selected $Fe^{II}(L)(H_2O)$ complexes

Complex	k_{ex} (s^{-1})	$\Delta H^{\ddagger}_{ex}$ (kJ mol^{-1})	$\Delta S^{\ddagger}_{ex}$ (J K^{-1} mol^{-1})	$\Delta V^{\ddagger}_{ex}$ (cm^3 mol^{-1})
$Fe^{II}(H_2O)_6$ [a]	4.4×10^{6}	41 ± 1	$+21\pm5$	$+3.8\pm0.2$
$Fe^{II}(mida)(H_2O)$	1.8×10^{7}	27 ± 3	-16 ± 11	$+1.2\pm0.2$ [b]
$Fe^{II}(mida)_2$ (H_2O)	2.4×10^{7}	39 ± 3	$+27\pm10$	$+3.2\pm0.2$ [b]

[a] Data from Ref. [28].
[b] Determined at 10 °C.

Table 3
Structural data on the $\{Fe–NO\}^{6/7}$ unit in nitrosylated haemoproteins and synthetic iron porphyrins

Fe(P)NO	Method	Fe–ligand distances (Å)		Fe–N–O angle (°)	Reference
		$Fe–N_{eq}$	Fe–NO		
{Fe–NO}^{7}					
$Mb^{II}(NO)$	MS XAFS	2.00	1.75	150	[29]
$Hb^{II}(NO)$	Crystal.	–	1.74	145	[30]
$Fe^{II}(OEP)(NO)$	Crystal.	2.01	1.73	143	[2]
$Fe^{II}(TPP)(NO)$	Crystal.	2.00	1.72	149	[2]
{Fe–NO}^{6}					
$Mb^{III}(NO)$	MS XAFS	2.00	1.68	180	[29]
P450nor-(NO)	MS XAFS	2.00	1.66	170	[31]
$[Fe^{III}(OEP)(NO)(H_2O)]$	Crystal.	1.99	1.64	177	[2]
$[Fe^{III}(TPP)(NO)(H_2O)]$	Crystal.	2.00	1.65	174	[34]

complex. Both these properties are controlled by the nature of L, which determines the electronic/structural features of a given Fe(II) chelate. Although these conclusions are based on a relatively narrow range of the complexes studied and should be evaluated in subsequent studies, the observed kinetic features of the $Fe^{II}(L)$–NO interactions are quite analogous to those observed in reactions of porphyrin-based complexes with NO (vide infra).

4. Interaction of NO with biomolecules

4.1. Myoglobin, haemoglobin and metmyoglobin

As in the case of non-haem iron proteins and their model complexes, metalloporphyrin nitrosyl adducts have long been investigated in relation to the studies on oxygen binding to haemoproteins which are responsible for transport and storage of oxygen, such as haemoglobin and myoglobin. Current scientific efforts in the area of NO–haem interactions, however, are mainly aimed at clarifying physiological effects which result from the interaction of NO with haemoproteins [1,5].

Nitric oxide reacts with both ferric and ferrous centres in haemoproteins to form the respective iron(II) and iron(III) nitrosyl adducts [1,29–33]. As can be seen from the data presented in Table 3, the structural features of these adducts are similar to those observed for iron(II) and iron(III) porphyrin nitrosyls [29–34]. These analogies are also reflected in similar chemical reactivity observed for nitrosylated ferri- and ferroproteins and their respective porphyrin models. For example, Fe^{III}–NO adducts which form upon NO binding to ferrihaem centres in metmyoglobin, methaemoglobin, ferricytochrome *c* and catalase, undergo reductive nitrosylation in the presence of excess NO [35], and similar process is commonly observed for synthetic Fe(III) porphyrins [2]. The first step of this reaction involves nucleophilic attack of OH^- on the nitrosyl ligand coordinated to the iron centre, as presented in Scheme 1.

Such reactivity of the nitrosylated protein ferrihaem demonstrates the formal NO^+ character of the nitrosyl ligand in the $\{Fe–NO\}^6$ unit, which has a similar electronic structure as in nitrosylated iron(III) porphyrins, viz. Fe^{II}–NO^+. In a similar way, formation of a typical $\{Fe–NO\}^7$ porphyrin nitrosyl upon binding of NO to the ferrohaem centre in the soluble guanylyl cyclase, can be deduced from the observed *trans*-labilisation effect [5], a characteristic feature of a nitrosyl ligand within the $\{Fe–NO\}^7$ porphyrin motif. It may, therefore, be concluded that ferri- and ferrohaem proteins tend to form $\{Fe–NO\}^6$ and $\{Fe–NO\}^7$ porphyrin nitrosyls, with a linear ($n = 6$) and bent ($n = 7$) geometry of the M–N–O group.

Despite the similarities in the nature of the nitrosyls in haemoproteins and model porphyrin systems, the kinetics of NO binding and dissociation from the porphyrin centres embedded in the protein usually differs from that observed for 'free' porphyrins. In fact, the rates of NO binding to various ferri- and ferrohaems, and water soluble porphyrins, vary over a range of more than eight orders of magnitude [1,36,37], as summarised in Table 4. Mechanistic studies on the origin of these differences in selected haemoproteins and model iron porphyrins have been reported in the literature [32,33], and the main factors which influence the dynamics of protein–NO interactions have been reviewed recently [1]. It has, in general, been concluded that the rates of nitrosylation observed for haemoproteins de-

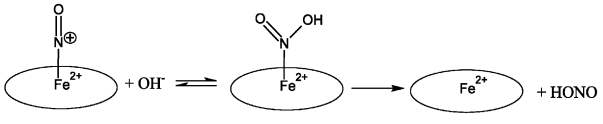

Scheme 1.

Table 4
Rate constants for the reversible nitrosylation of representative haemoproteins and model porphyrins

Fe(P)	Conditions [a]	k_{on} ($M^{-1} s^{-1}$)	k_{off} (s^{-1})	K_{NO} ($=k_{on}/k_{off}$)	References
Fe(III)					
Mb^{III}	pH 7.4	4.74×10^{4}	37.4	1.3×10^{3}	[33]
Cat^{III}	pH 6.5	3.0×10^{7}	1.7×10^{2}	1.8×10^{5}	[1]
Cyt c^{III}	pH 6.5	7.2×10^{2}	4.4×10^{-2}	1.6×10^{4}	[1]
Fe^{III}(TPPS)	pH 6.5	7.2×10^{5}	6.8×10^{2}	1.1×10^{3}	[1]
Fe^{III}(TMPS)	pH 6.0	3.0×10^{6}	7.3×10^{2}	4.1×10^{3}	[36]
Fe(II)					
Hb^{II}	pH 7.0	2.5×10^{7}	4.6×10^{-5}	5.3×10^{11}	[1]
Mb^{II}	pH 7.0	1.7×10^{7}	1.2×10^{-4}	1.4×10^{11}	[1]
Cyt c^{II}	H_2O	8.3	2.9×10^{-5}	2.9×10^{5}	[32]
Fe^{II}(PP)(1-MeIm)	pH 9.0	1.8×10^{8}	2.9×10^{-4}	6.2×10^{11}	[1]
Fe^{II}(TPPS)	pH 7.0	1.5×10^{9}	<2		[37]
Fe^{II}(TMPS)	pH 7.0	1.0×10^{9}	–		[37]
Fe^{II}(TPP)	Toluene	5.2×10^{9} [b]	4.17×10^{-5} [c]	1.2×10^{14}	[1], [40]
Fe^{II}(OETAP)	Toluene	–	0.15 [c]		[41]
Fe^{II}(OBTPP)	Toluene	–	47 [c]		[40]

[a] Values measured at 25 °C unless otherwise noted.
[b] From Ref. [1].
[c] Determined by displacement of NO by a nitrogen base (*N*-methylimidazole or pyridine).

pend in part on the protein structure, the conformation and the nature of ligands in the proximity of the metal centre being of special importance. In these cases where the protein limits access of NO to the metal site, the rates of the 'on' reactions for both Fe(II) and Fe(III) centres are slow [32,38]. However, when such access is facile, the 'on' reaction is dominated by the reactivity of the metal centre. The fast rates of NO binding observed in such cases reflect the lability of the high-spin iron(II) and iron(III) porphyrins [36,37,39].

Dissociation of NO from nitrosylated haemoproteins is in general hindered by the presence of the protein surrounding. Apart from this effect, a variety of other factors, related mainly to the nature of the Fe–NO bond in the protein haem nitrosyl, apparently affect the kinetics of NO release. As can be seen from the data in Table 4, ferrihaem nitrosyls are in most cases considerably more labile toward NO dissociation than their ferrohaem analogues. This indicates that the iron oxidation state is an important factor that affects the rate of NO loss from the (porphinato)iron nitrosyl. In terms of the Enemark and Feltham formalism, it may be concluded that the iron-nitrosyl bond within a bent $\{Fe–NO\}^7$ unit is more stable toward NO dissociation than the corresponding bond in a linear $\{Fe–NO\}^6$ unit. Such an effect presumably results from specific bonding interactions of the iron(II) centre with the nitrosyl ligand, which are reflected in characteristic structural distortions observed within the $\{Fe–NO\}^7$ unit in nitrosylated iron(II) porphyrins [2,8].

Detailed studies on synthetic Fe^{II}(P)NO complexes revealed the strong influence of electronic and stereochemical properties of porphyrin substituents on the rate of NO release [40,41]. Despite the similar structural features of the iron–nitrosyl group in all the complexes studied, dramatic differences in the rates of NO release were observed, apparently due to variations in the electronic structure within the $\{Fe–NO\}^7$ unit. However, the electronic factors that mainly influence the stability of the Fe^{II}–NO bond remain to be clarified. Mössbauer spectroscopy and theoretical calculations appear to be the most promising techniques in this respect [9,10,40].

From a mechanistic perspective, studies on the NO release from iron(II) porphyrin nitrosyls are often complicated by inconveniently slow kinetics of these processes. It is therefore difficult to obtain information on the mechanism of NO dissociation from the $\{Fe–NO\}^7$ unit. This contrasts the kinetic behaviour of iron(III) porphyrin centres, where both association and dissociation of NO are usually easily observable under physiological conditions. Kinetic studies on these processes give an opportunity to gain insight into the mechanisms for the formation and decay of ferrihaem nitrosyls. As a consequence, more is known about the nature of the Fe–NO bond in iron(III) nitrosyls, and on the process of NO release from these complexes. This can be illustrated by recent mechanistic studies on the reversible binding of NO to metmyoglobin [33]. As in the case of model iron(III) porphyrins, the high-spin Fe(III) centre of metmyoglobin is six-coordinate, with a labile water molecule occupying the potential coordination site of NO. The binding of NO to the iron porphyrin centre of the protein is given by reaction (3).

$$\mathrm{metMb(H_2O)} + \mathrm{NO} \underset{k_{off}}{\overset{k_{on}}{\rightleftarrows}} \mathrm{metMb(NO)} + \mathrm{H_2O} \qquad (3)$$

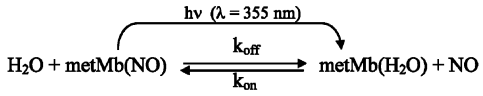

Scheme 2.

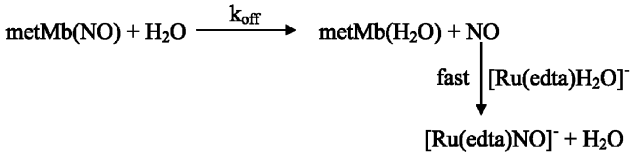

Scheme 3.

FTIR and MS XAFS data [29,42] have shown that the reaction product, metMb(NO), is a linear {Fe-NO}^{6} nitrosyl which formally has Fe^{II}–NO^+ character, i.e. partial charge transfer from NO to Fe(III) occurs during the binding process. The equilibrium constant for reaction (3) determined by spectrophotometric titration in aqueous medium [33] was found to be 2.4×10^3 M^{-1}. In an excess of NO, the reaction follows pseudo-first order kinetics, and the observed rate constant is a linear function of [NO], as given in Eq. (4).

$$k_{obs} = k_{on}[NO] + k_{off} \quad (4)$$

The rates of the binding and release of NO in this system can be conveniently measured either by stopped-flow mixing of aqueous metMb(H_2O) and NO solutions, or by flash photolysis of equilibrium mixtures of metMb and metMb(NO). In the latter case, the system is displaced from equilibrium by a laser flash (see Scheme 2), and the kinetics of the relaxation back to the equilibrium position can be followed spectrophotometrically.

The values of k_{on} and k_{off} were determined from the slopes and intercepts of linear plots of k_{obs} versus [NO], obtained from the stopped-flow and laser flash photolysis experiments. The k_{off} values obtained in this way were confirmed more directly by application of an NO-trapping method. This involved rate-determining loss of NO from metMb(NO) using an excess of $[Ru^{III}(edta)H_2O]^-$ as an NO-scavenger as shown in Scheme 3.

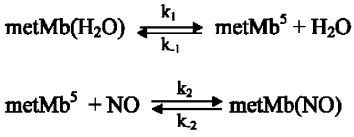

Scheme 4.

Activation parameters ($\Delta H^{\ddagger}$, $\Delta S^{\ddagger}$and $\Delta V^{\ddagger}$) for the 'on' and 'off' reactions were obtained from systematic measurements of k_{on} and k_{off} as a function of temperature (5–45 °C) and pressure (0.1–130 MPa). As can be seen from the kinetic data summarised in Table 5, the results obtained for both reactions using the fundamentally different stopped flow and laser flash photolysis techniques, are in good agreement. Activation parameters reported in the table indicate that both the forward and back reactions exhibit large and positive values for $\Delta S^{\ddagger}$ and $\Delta V^{\ddagger}$. Such results clearly show that both processes (i.e. binding and release of NO) follow a dissociative ligand substitution mechanism as depicted in Scheme 4, where metMb^5 is a five-coordinate intermediate formed by the dissociation of H_2O from metmyoglobin.

According to this mechanism, the rate-determining steps for the 'on' and 'off' reactions (k_1 and k_{-2}, respectively) involve the dissociation of H_2O and NO from the first coordination sphere of the iron centre, respectively. The forward reaction exhibits a large activation enthalpy indicative of the relatively high energy required to break the Fe^{III}–OH_2 bond. Large positive values for $\Delta S^{\ddagger}_{on}$ and $\Delta V^{\ddagger}_{on}$ are in line with the dissociation of water molecule from the metMb(H_2O) complex in the absence of any significant changes in solvation.

The reverse process dominated by the k_{-2} step (i.e. dissociation of NO), involves homolysis of the Fe–NO bond within a diamagnetic {Fe–NO}^{6} unit with a formal Fe^{II}–NO^+ character to give a paramagnetic, high-spin Fe^{III}(porphyrin)H_2O centre and free NO. Activation parameters for this step reflect the intrinsic entropy and volume changes associated with bond breakage, solvent reorganisation during charge redistribution, and a low-spin to high-spin transformation at the iron centre. Contributions from these processes are expected to give overall large and positive values for $\Delta S^{\ddagger}_{off}$ and $\Delta V^{\ddagger}_{off}$ as observed for metMb(NO).

Table 5
Rate constants and activation parameters for the binding of NO to metMb(H_2O) (k_{on}) and release of NO from metMb(NO) (k_{off}) determined by laser flash photolysis and stopped flow techniques [a]

Experimental method	k_{on} [b] (M^{-1} s^{-1})	k_{off} [b] (s^{-1})	$\Delta H^{\ddagger}_{on}$ (kJ mol^{-1})	$\Delta S^{\ddagger}_{on}$ (J mol^{-1} K^{-1})	$\Delta V^{\ddagger}_{on}$ (cm^3 mol^{-1})	$\Delta H^{\ddagger}_{off}$ (kJ mol^{-1})	$\Delta S^{\ddagger}_{off}$ (J mol^{-1} K^{-1})	$\Delta V^{\ddagger}_{off}$ (cm^3 mol^{-1})
Laser flash	4.7×10^4	37	63 ± 2	55 ± 8	20 ± 6	68 ± 4	14 ± 13	18 ± 3
Stopped-flow	4.8×10^4	29	63 ± 4	54 ± 14	21 ± 1	65 ± 5	3 ± 16	16 ± 1
NO-trapping		24				78 ± 2	46 ± 7	20 ± 1

[a] Data from Ref. [33].
[b] Determined at 25 °C, pH 7.4.

Table 6
Activation parameters for the binding of NO to $Fe^{III}(P)(H_2O)_2$ (k_{on}), the dissociation of NO from $Fe^{III}(P)(H_2O)(NO)$ (k_{off}), and water exchange on model $Fe^{III}(P)(H_2O)_2$ complexes

	$Fe^{III}(TPPS)(H_2O)_2$			$Fe^{III}(TMPS)(H_2O)_2$		
	$\Delta H^{\ddagger}$ (kJ mol^{-1})	$\Delta S^{\ddagger}$ (J mol^{-1} K^{-1})	$\Delta V^{\ddagger}$ (cm^3 mol^{-1})	$\Delta H^{\ddagger}$ (kJ mol^{-1})	$\Delta S^{\ddagger}$ (J mol^{-1} K^{-1})	$\Delta V^{\ddagger}$ (cm^3 mol^{-1})
$Fe(P)(H_2O)_2+NO$ *NO binding* [a]	70 ± 3	$+100 \pm 4$	$+8.3 \pm 1.5$	62 ± 2	$+86 \pm 2$	$+13 \pm 1$
$Fe(P)(H_2O)_2+H_2O$ *water exchange* [b]	67 ± 2	$+99 \pm 10$	$+7.9 \pm 0.2$	61 ± 1	$+100 \pm 5$	$+11.9 \pm 0.3$
$Fe(P)(H_2O)(NO)$ *NO release* [a]	78 ± 4	$+67 \pm 3$	$+17.9 \pm 1.4$	83 ± 3	$+89 \pm 3$	$+18 \pm 4$

[a] Data from Ref. [36].
[b] Data from Ref. [39].

The proposed dissociative mechanism for the reversible binding of NO to metMb is supported by earlier studies on water-soluble model iron(III) porphyrins, $Fe^{III}(TPPS)$ and $Fe^{III}(TMPS)$ complexes [36]. As can be seen from the data presented in Table 6, mechanistic features exhibited by the model iron porphyrin complexes in their reactions with NO are very similar to that observed for metmyoglobin. In addition, kinetic data for water exchange on $Fe^{III}(TPPS)(H_2O)_2$ and $Fe^{III}(TMPS)(H_2O)_2$ are in excellent agreement with this mechanistic interpretation [39]. Large and positive $\Delta S^{\ddagger}_{ex}$ and $\Delta V^{\ddagger}_{ex}$ values demonstrate the dissociative nature of the water exchange process and are very similar to that observed for the respective nitrosylation reaction. In fact, the activation volume reported for the binding of NO to $Fe^{III}(TPPS)(H_2O)_2$ [38] is identical to that found for water exchange on this complex [39], indicating that the binding of NO is controlled by the water exchange reaction on the Fe(III) centre.

A comparison of the volume profiles for the reaction of NO with $metMb(H_2O)$ and $Fe(TPPS)(H_2O)_2$ reported in Fig. 4, clearly illustrates the similar mechanistic behaviour of metMb and model iron(III) complexes. However, whereas the $\Delta V^{\ddagger}_{on}$ value observed for the binding of NO to $Fe^{III}(TPPS)(H_2O)_2$ is close to the maximum volume increase of 13 cm^3 mol^{-1} expected for the dissociation of a water molecule from an octahedral complex [43,44], the $\Delta V^{\ddagger}_{on}$ value obtained for the reaction of NO with metMb is significantly larger. This observation was interpreted in terms of a structural rearrangement of the protein upon release of coordinated water prior to the binding of NO, which leads to a further increase in the size of the protein in the transition state. This conclusion is in line with XAFS structural data on nitrosylated metMb [29], which indicate steric strain in the linear coordination of NO to the Fe(III) centre, and thus support the contention that an increase in the size of the protein pocket occurs prior to the binding of NO.

4.2. Cytochrome c^{II} and c^{III}

As mentioned in the previous section, the protein environment may affect significantly the kinetics of the binding of NO to the haem centre in haemoproteins. This can be illustrated by the reaction of NO with the ferric and ferrous forms of cytochrome *c*, a haem-containing mitochondrial protein involved in electron transfer processes during biological oxidations.

Structural data on Cyt *c* revealed that the fifth and sixth coordination sites at the metal haem centre are occupied by histidine and methionine residues in both oxidation states of the protein [1,38]. As a consequence, a very labile coordination site (such as that present in the high-spin iron(III) and iron(II) centres of myoglobin, haemoglobin and model iron porphyrins) is not available. Thus, coordination of NO to cytochrome *c* involves in this case the displacement of a relatively tightly bound axial ligand (i.e. methionine or histidine). As a consequence, an unusually slow rate for NO binding to the iron porphyrin centre in Cyt c^{III} and Cyt c^{II} is observed (see data in Table 4). In particular, the rate constant observed for the binding of NO to the Fe(II) haem centre of ferrocytochrome *c* is significantly *smaller* than that for the corresponding ferric form, i.e. k_{on} (Cyt c^{II}) $\ll k_{on}$ (Cyt c^{III}). These results contradict the

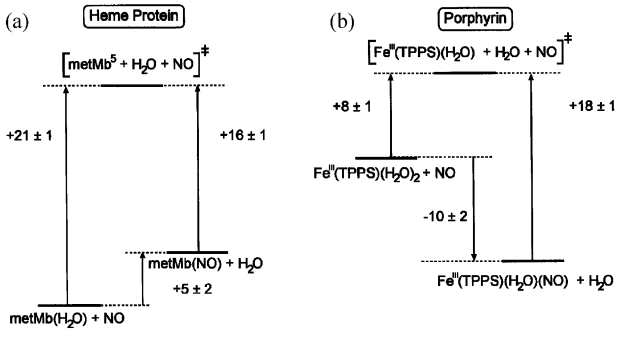

Fig. 4. Volume profiles for the reversible binding of NO to $metMb(H_2O)$ and $Fe^{III}(TPPS)(H_2O)_2$.

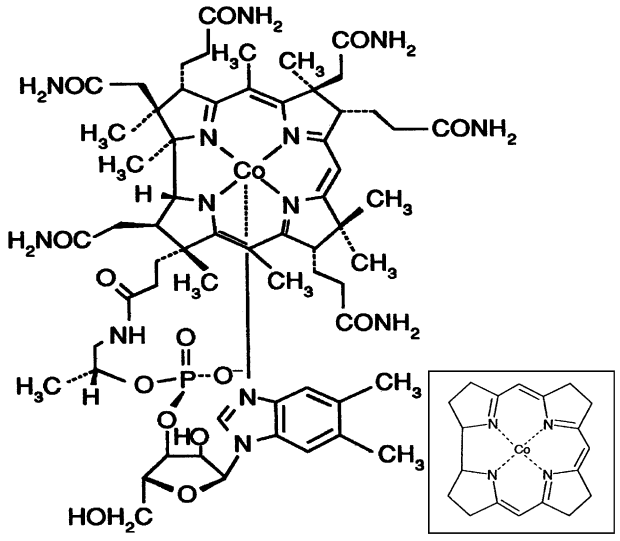

Fig. 5. Structure of reduced vitamin B_{12} (cob(II)alamin) at pH > 3. Inset: schematic structure of the cobalt corrin ring.

general reactivity trend observed for model Fe(II) and Fe(III) porphyrins (see Table 4) and apparently reflect the stronger binding of the axial ligands in the reduced form of the protein [32,38].

Despite the differences in the kinetics of NO binding to the ferric and ferrous form of cytochrome *c*, compared to that observed for model iron(II) and iron(III) porphyrins, the resulting protein nitrosyls exhibit typical structural and chemical features of the $\{Fe–NO\}^6$ and $\{Fe–NO\}^7$ porphyrin adducts. This can, for instance, be illustrated with the NO^+ character of the nitrosyl ligand within the $\{Fe–NO\}^6$ unit formed in the nitrosylated ferricytochrome *c*, which undergoes reductive nitrosylation in a similar manner as the other $\{Fe–NO\}^6$ nitrosyl porphyrinates [35]. It follows that the kinetics of NO binding to both forms of cytochrome *c*, although significantly different from that observed for labile iron(II) and iron(III) porphyrins, is still controlled by the lability of the metal–ligand system. The free-radical nature of NO does not have a significant influence on the observed reaction dynamics, and the reaction leads to the formation of typical $\{Fe–NO\}^{6/7}$ nitrosyls.

4.3. Reduced vitamin B_{12}

Reduced vitamin B_{12} (cob(II)alamin, Cbl(II)), a naturally occurring cobalt(II) macrocyclic complex belongs to the class of vitamin B_{12} derivatives, which play a vital role in several enzymatic biotransformations. The common structural feature of these relatively complex biomolecules is the presence of the equatorial corrin chelate coordinated to the cobalt atom, as shown in Fig. 5. The sixth coordination position in vitamin B_{12} derivatives containing cobalt in the +3 oxidation state, can be occupied by various ligands (such as H_2O in aquacobalamin, $Cbl(III)H_2O$), while in the case of reduced vitamin B_{12} the sixth coordination site of the low-spin cobalt(II) centre remains vacant [45,46].

The structure of the corrin (see inset in Fig. 5) is similar to that of a porphyrin, but lacks one of the bridging methylene groups in the tetrapyrrolic ring. As a result, the corrin ring is more flexible (due to the partial loss of aromaticity of the tetrapyrrole ring)[47,48] and has a smaller cavity size compared to that of a porphyrin ring [47]. Despite these differences, the main structural and electronic features of corrins are relatively similar to that of porphyrins.

One of the recent interests in the chemistry and biochemistry of vitamin B_{12} derivatives concerns the interaction of aquacobalamin ($Cbl(III)H_2O$) and its reduced form (Cbl(II)) with NO [49–54]. The physiological effects observed which provide evidence for cobalamin–NO interactions in vivo were interpreted originally in terms of the NO binding to aquacobalamin, as shown in reaction (5) [49,50].

$$Cbl(III)H_2O + NO \rightleftarrows Cbl(III)NO + H_2O \quad (5)$$

Detailed spectroscopic and kinetic studies, however, failed to provide convincing evidence for the formation of the Cbl(III)NO complex [51–53]. The UV–Vis spectral changes observed on introducing NO into aqueous solutions of $Cbl(III)H_2O$, have been shown to result from the reaction of Cbl(III) with nitrite (present as an impurity in aqueous NO solutions) according to reaction (6), rather than from the reaction of aquacobalamin with NO [53] (see also Section 5.1).

$$Cbl(III)H_2O + NO_2^- \overset{K}{\rightleftarrows} Cbl(III)(NO_2^-) + H_2O \quad (6)$$

Notably, on considering the similarity between the corrin and porphyrin ligands, binding of NO to the Co(III) centre of $Cbl(III)H_2O$ would lead to the formation of a porphyrin-like $\{M–NO\}^7$ nitrosyl. However, stable porphyrin nitrosyls with this electronic configuration have only been obtained for iron(II) porphyrins [2,8], from which it follows that the $\{Co^{III}–NO\}^7$ complex is not likely to form. On the contrary, UV–Vis, NMR and resonance Raman spectroscopic studies clearly indicate that the reduced form of vitamin B_{12} reacts with NO to form a stable nitrosyl complex [50,52,54], according to the overall reaction (7).

$$Cbl(II) + NO \overset{K}{\rightleftarrows} Cbl(II)NO \quad (7)$$

Formation constants for this complex, viz. $K = 1.0 \times 10^8\ M^{-1}$ at pH 7.0 [52], and $K = 3.1 \times 10^7\ M^{-1}$ at pH 7.4 [54], have been reported recently by two different research groups. These values indicate that the binding of NO by cob(II)alamin is very efficient, and thus may account for the observed physiological effects.

In terms of the Enemark and Feltham notation, the Cbl(II)NO complex belongs to the class of the

{M–NO}^{8} species. As mentioned in Section 2.1, metalloporphyrin nitrosyls of this electronic configuration exhibit the general structural features shown in Fig. 1c. In particular, a bent M–N–O group ($\angle$(M–N–O) $\approx$ 120°) and a strong *trans*-labilising effect of the NO ligand are typical properties observed for this class of compounds. Although the crystal structure of nitrosylcob(II)alamin has not yet been reported, the presence of a strongly bent M–N–O group, similar to that observed in {M–NO}^{8} metalloporphyrins, has been confirmed by ^{15}N-NMR spectroscopy [54]. In addition, significant weakening of the bond between the cobalt centre and the nitrogen donor of dimethylbenzimidazole upon binding of NO to Cbl(II), demonstrates the strong *trans*-labilising effect of the bound nitrosyl ligand [54]. It follows that the Co(N_{eq})NO coordination group in nitrosylcob(II)alamin exhibits similar properties to that observed for typical {M–NO}^{8} nitrosylporphyrins. Notably, the well-resolved ^{15}N-NMR and ^{1}H-NMR spectra of nitrosylated cob(II)alamin [54] indicate the low-spin diamagnetic character of the complex, resulting from the combination of the unpaired electron of the paramagnetic d^7 Co(II) centre with the odd electron residing on the π^* orbital of NO. This process can be looked upon as a formal oxidation of the Co(II) centre with formation of a Cbl(III)(NO$^-$) species [12]. Thus, the binding of NO to cob(II)alamin is summarised in Scheme 5.

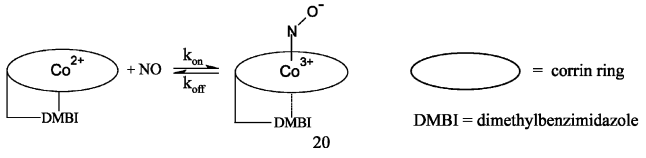

20

Scheme 5.

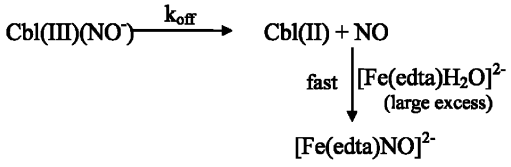

Scheme 6.

Table 7
Rate constants and activation parameters for the binding and release of NO from cob(II)alamin

Kinetic parameter	Forward reaction	Back reaction
Rate constant [a]	7.4×10^8 M^{-1} s^{-1}	5.6 s^{-1}
$\Delta H^{\ddagger}$ (kJ mol^{-1}) [b]	24.5 ± 0.7	76 ± 1
$\Delta S^{\ddagger}$ (J mol^{-1} K^{-1}) [b]	$+7 \pm 2$	$+24 \pm 5$
$\Delta V^{\ddagger}$ (cm^3 mol^{-1}) [a]	$+5.4 \pm 0.2$	$+7.9 \pm 0.5$

[a] 25 °C, pH 7.4.
[b] pH 7.4.

It may be expected that the formation and decay of the corrin {Co–NO}^{8} nitrosyl should be governed by similar general rules that determine the reactivity of nitric oxide towards metal centres in metalloporphyrins. The kinetics and mechanism of NO binding to cob(II)alamin should thus be determined by the lability of the Co(II) centre, whereas NO dissociation from the corrin {Co–NO}^{8} nitrosyl should reflect the properties of the Co(III)–NO$^-$ bond. In this respect, detailed kinetic studies on the 'on' and 'off' reaction have been performed in our laboratories in order to gain insight into the mechanisms of these reactions in the studied system [54]. The kinetics of NO binding to cob(II)alamin was studied with the use of laser flash photolysis under pseudo-first order conditions with respect to NO. Irradiation of the Cbl(III)(NO$^-$) complex with a laser beam in aqueous solution led to the formation of Cbl(II) and free NO. Following the flash, re-formation of Cbl(III)(NO$^-$) complex could be observed. The reaction sequence induced by the laser flash can therefore be expressed as in reaction (8).

$$\text{Cbl(III)NO}^- \xrightarrow{h\nu\ (532\ \text{nm})} \text{Cbl(II)} + \text{NO} \overset{k_{on}}{\rightarrow} \text{Cbl(III)(NO}^-) \quad (8)$$

The decay of the transient spectrum of the photo-induced Cbl(II) species in the presence of excess NO enables the measurement of the pseudo-first order rate constant for the formation of the Co–NO bond, k_{obs}, as a function of [NO].

$$k_{obs} = k_{on}[\text{NO}] + k_{off} \quad (9)$$

In contrast to the reversible binding of NO to metmyoglobin (see Section 4.1), no measurable intercepts were observed in the linear plots of the k_{obs} versus [NO] in the present system. This indicates that the k_{off} values characterising the back reaction are too small to be observed in the laser flash experiments. It was, however, possible to measure k_{off} directly using an NO-trapping technique. This involved rapid mixing of the Cbl(III)(NO$^-$) solution with high concentrations of [Fe^{II}(edta)H$_2$O]$^{2-}$ (used as a scavenger for NO) in a stopped flow instrument. Under such conditions, dissociation of NO from nitrosylated cob(II)alamin occurs as shown in Scheme 6.

At a sufficiently high concentration of [Fe(edta)H$_2$O]$^{2-}$, dissociation of NO from Cbl(III)(NO$^-$) becomes the rate-determining step, such that $k_{obs} = k_{off}$. The 'on' and 'off' rate constants and the corresponding activation parameters, $\Delta H^{\ddagger}$, $\Delta S^{\ddagger}$ and $\Delta V^{\ddagger}$ determined from the temperature and pressure dependence of k_{on} and k_{off}, are summarised in Table 7.

It is reasonable to expect that binding of NO to the vacant coordination site of the five-coordinate cobalt(II) centre in reduced vitamin B$_{12}$ should be fast. Such a process could be either controlled by diffusion of NO, or by the formation of the Co–NO bond. In the

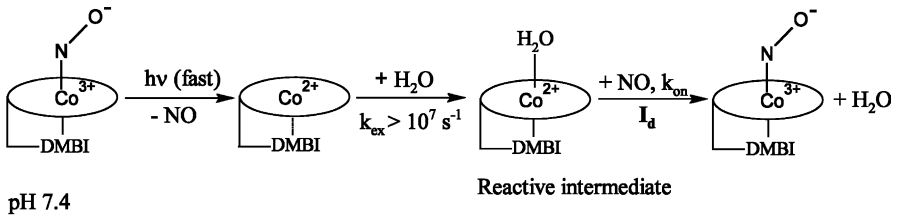

Scheme 7.

latter case the reaction should exhibit a significantly negative activation volume due to bond formation and formal oxidation of the Co(II) centre in the rate-determining step. As can be seen from the kinetic data obtained for the 'on' reaction (see Table 7), these expectations are not in line with experimental observations. Although the observed reaction is very fast, it is approximately two orders of magnitude slower than the limiting rate constant for a diffusion-controlled reaction in water ($k_d \sim 10^{10}$ $M^{-1} s^{-1}$ at 298 K) [55] and, surprisingly, exhibits a small but significantly positive volume of activation, viz. $+5.4$ $cm^3 mol^{-1}$. This value cannot be correlated with a simple bond formation process at the vacant coordination site of cob(II)alamin, but provides evidence for the operation of a dissociative interchange (I_d) ligand substitution mechanism for the photo-induced 'on' reaction [43,56]. It follows that the rate-determining step in the binding of NO apparently involves displacement of water at the Co(II) centre in the photo-induced reactive Cbl(II) intermediate.

A detailed investigation of this system [54] has shown that the above conclusion, although rather surprising at first sight, can be reconciled with the general reactivity patterns observed in the reactions of nitric oxide with metal centres. A thorough study of the transient spectra recorded immediately after the laser flash, revealed that the reactive Cbl(II) intermediate generated in aqueous medium, differs from the intact Cbl(II) species which binds NO in the thermal reaction. According to the most self-consistent reaction scheme based on all spectroscopic and kinetic measurements performed for the system studied [54], photo-dissociation of NO from nitrosylcob(II)alamin leads to the formation of a five-coordinate Cbl(II) species with a weakly coordinated DMBI ligand, as shown in Scheme 7. This species rapidly binds a water molecule prior to the recombination with NO, forming an aqua intermediate. Binding of NO to this intermediate is controlled by displacement of the very labile water molecule according to an I_d mechanism, and accounts for the positive volume of activation found for the 'on' reaction. Such a water molecule is, however, not present in the intact cob(II)alamin complex at physiological pH [57], such that the intimate reaction mechanisms are expected to differ for the photo-induced and thermal nitrosylation of reduced cobalamin. The latter process is presumably controlled by NO binding to the vacant coordination site on the intact Cbl(II) complex and is expected to be even faster than the corresponding photo-induced reaction, where the binding of NO involves substitution of coordinated water on the photo-generated Cbl(II) species.

Kinetic data for the 'off' reaction summarised in Table 7 clearly indicate that the dissociation of NO from nitrosylcob(II)alamin is slow, and a high energy barrier (reflected in a large $\Delta H^{\ddagger}_{off}$ term) must be overcome to break the Co(III)–NO^- bond in the $\{Co–NO\}^8$ corrin nitrosyl. A positive activation volume observed for this process can be accounted for in terms of a dissociative interchange mechanism in which the breakage of the Co–NO bond is accompanied partially by the strengthening of the Co–N(DMBI) bond in the position *trans* to the leaving nitrosyl ligand.

Due to the fact that the reactive Cbl(II) intermediates in the thermal and photo-induced 'on' reactions are not the same, the data presented in Table 7 do not allow construction of energy and volume profiles for the overall reaction shown in Scheme 6. It is, however, possible to construct a volume profile for the binding of NO to the photo-generated aqua complex at pH 7.4, as shown in Fig. 6. The volume profile once again illustrates the I_d character of the 'on' and 'off' reactions and the important role of solvent molecules in determining the mechanism of NO binding to the metal centre.

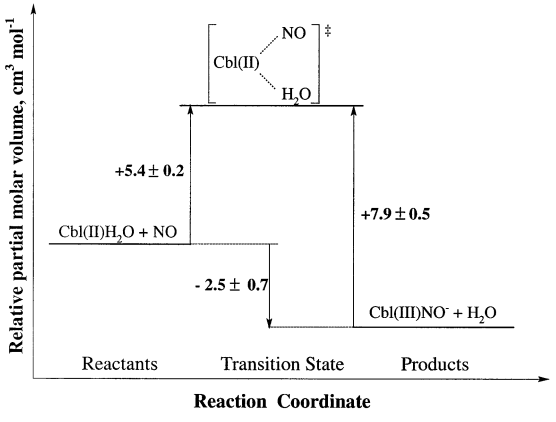

Fig. 6. Volume profile for the photo-induced reaction $Cbl(II)H_2O + NO \rightleftharpoons Cbl(III)(NO^-) + H_2O$.

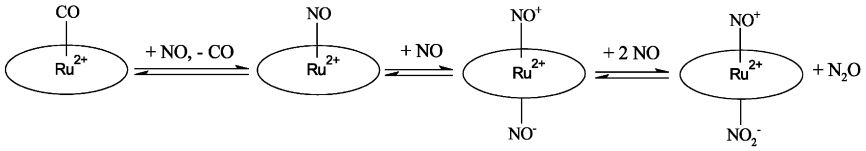

Scheme 8.

5. Problems in the study of reactions of NO with metal complexes in solution

5.1. Is the reactive species NO or NO_2^-/HONO?

Various studies on the mechanism of the interaction of NO with inorganic and bioinorganic metal complexes have encountered the complex redox solution chemistry of NO, which often posed experimental difficulties in the study of such reactions [5,58]. From a biological perspective, the interaction of NO with different species such as molecular oxygen, superoxide and transition metal ions under biological conditions can result in the formation of a variety of oxidation and reduction products with discrete biological activities. The contribution of such species to the observed NO reactivity is sometimes not realised and may therefore lead to difficulties in the correlation of data on the reactivity of NO obtained in vitro with the measurable biological effects. In order to contribute to the clarification of such effects, we now focus on the central question of this review (To be or not to be NO in coordination chemistry?) in terms of the identity of the actual reactive species in solution.

Important complications that may affect kinetic studies on the interaction of NO with metal centres arise from the facile oxidation of NO by molecular oxygen in solution to produce NO_2 and N_2O_3 (formed from NO_2 and excess NO). In aqueous solution, this process leads to the formation of nitrite ions [58] according to reactions (10)–(12) and, unless care

$$NO_2 + NO \rightleftarrows N_2O_3 \quad (10)$$

$$N_2O_3 + H_2O \rightarrow 2HONO \quad (11)$$

$$HONO \rightleftarrows H^+ + NO_2^- \quad (12)$$

is taken, may lead to significant contamination of the aqueous solutions of NO with NO_2^-/HONO [53]. Although this complication can to some extent be avoided by the preparation and handling of NO solutions under strictly oxygen-free conditions, and by removing the higher nitrogen oxides from the NO gas stream [53,59], it is practically impossible to completely eliminate contamination of aqueous solutions of NO by traces of nitrite. Based on our own experience, NO saturated aqueous solutions prepared under an inert atmosphere may easily contain nitrite in a concentration range of 0.3–3 mM [53]. Such a contamination can be detected in a relatively simple way by monitoring the characteristic fingerprint UV–Vis spectrum of HONO, recorded following the acidification of the NO solution to pH 2 [53].

The possible interference of NO_2^-/HONO or higher nitrogen oxides (as found in aprotic media, see below) in the reactions observed should be kept in mind on considering the extensive, and sometimes controversial, data available in the literature concerning the mechanism of NO interactions with metal complexes.

It may be sometimes difficult to distinguish the reaction of NO from that caused by the interference of NO_2 and N_2O_3 present as contaminants in the aprotic solvent saturated with NO. This can be illustrated by recent studies on the reaction of selected Ru(II) and Fe(II) porphyrinates with NO. Porphyrin carbonyl complexes of the type $M^{II}(P)(CO)$ (where $M = Ru^{II}$ or Fe^{II} and P = various porphyrins), have been shown to react with excess NO in aprotic solvents, such as toluene and chloroform, to form nitrosyl nitro complexes, $M(P)(NO)(NO_2)$ [59–62]. Despite the analogy of the final products formed by the ruthenium and iron analogues, different reactivity patterns for these two metals have been suggested [59]. In the case of the Ru^{II} porphyrins, a metal-assisted disproportionation reaction, in which the initially formed nitrosyl complex reacts further with NO (see Scheme 8), is rather well established [61,62].

On the contrary, the analogous $Fe^{II}(TPP)(NO)(NO_2)$ complex was claimed to be formed only in the presence of NO_2/N_2O_3 impurities in the reaction medium [59], and the process outlined in Scheme 9 was suggested as the only reaction path leading to the formation of the iron(II) nitrosyl nitro complex.

This conclusion is, however, difficult to reconcile with the results of more recent studies on the reactivity of $Fe^{II}(TPP)CO$ with NO reported by another group, which suggest that the reactivity patterns of ruthenium(II) and iron(II) porphyrinates with excess NO are in fact similar [60]. Despite the sophisticated studies on the intimate reaction mechanism [60], the nature of the reactive species in solution and the identity of the intermediates occurring in the reaction of iron(II) porphyrins in the presence of excess NO is not fully clarified.

Similarly, experimental difficulties may arise from contamination of aqueous NO solutions with nitrite

ions. This can be illustrated by studies on the apparent interaction of nitric oxide with aquacobalamin, which was reported to act as a possible scavenger for NO in biological systems [49–51]. Experimental observations, originally interpreted in terms of the binding of NO to aquacobalamin, have in the meantime been shown to result from the reaction of aquacobalamin with nitrite ions present as impurity in aqueous NO solutions [53].

Although the interfering reactions with nitrite are in many cases much slower than those with NO, and as such do not directly interfere with the reaction kinetics observed (see below), they may change the chemical nature of the sample solution with time and, in some cases, lead to erroneous or irreproducible results. Thus, additional control is necessary in order to show that nitrite is not an interference in the system under investigation. Due to the possibility of such interference, a study and description of the differences between the reactivity of nitric oxide and nitrite towards metal centres forms an important aspect of investigations on metal–NO interactions in inorganic systems. Such studies are also of biological interest, considering the fact that nitrite is the major product of NO metabolism, such that nitric oxide and nitrite are two metabolically related species present in body fluids.

5.2. Interactions of nitrite with transition metal complexes

Nitrite can react with metal centres in different ways. Many of these reactions involve coordination of nitrite to the metal centre. This may lead to the formation of a stable nitro complex, or occur as an initial step followed by subsequent reactions of the coordinated nitrite ligand, such as intramolecular M–ONO to M–NO_2^- isomerisation, oxygen transfer [63,64], nitro/nitrosyl interconversion [13,65,66], nucleophilic addition and reduction processes [32,67–70]. In addition, due to the relatively high redox potential of NO_2^- and, in particular of its conjugated acid HONO, interaction of NO_2^-/HONO with metal centres may involve oxidation of the metal with simultaneous reduction of NO_2^- (or HONO) to nitric oxide [71]. These processes may interfere in the studies on NO interactions with metal complexes when nitrite ions are present as impurities in the sample. Their importance, however, strongly depends on the system studied and experimental conditions applied in a particular study. Although nitrite can react with a large number of transition metal complexes, the present review concerns mainly metalloporphyrin and chelate iron(II) complexes. In this respect, some important aspects of nitrite interactions with metal centres in such complexes will be presented and discussed on the basis of selected examples.

Extensive studies on the interactions of iron porphyrins with nitrite ions in non-aqueous solvents has shown that nitrite is a relatively strong ligand toward iron porphyrinates [64,72–77]. Coordination of nitrite to synthetic iron(III) porphyrins results in formation of the low spin, usually six-coordinate bis-nitro or mixed ligand complexes, as shown in reactions (13) and (14) [77].

$$Fe^{III}(P)(X)_2 + NO_2^- \rightleftarrows Fe^{III}(P)(X)(NO_2^-) + X^- \quad K_1 \tag{13}$$

$$Fe^{III}(P)(X)(NO_2^-) + NO_2^- \rightleftarrows Fe^{III}(P)(NO_2^-)_2 + X^- \quad K_2 \tag{14}$$

The resulting nitrite complexes, however, can easily undergo subsequent reactions to yield the iron(II) nitrosyl derivatives, $Fe^{II}(P)(X)(NO)$ and $Fe^{II}(P)(NO_2^-)(NO)$, as the final reaction products [64,72,77]. Although the structural and electronic features of the resulting complexes are well characterised [64,75], the suggested reaction pathways which lead to their formation remains controversial [77]. The most often invoked mechanism which accounts for the formation of iron(II) porphyrin nitrosyls from the respective iron(III) nitrite complexes involves an oxygen atom transfer from coordinated nitrite to various oxygen acceptors, including NO_2^-, as shown in reaction (15).

$$Fe^{III}(P)(X)(NO_2^-) + NO_2^- \rightleftarrows Fe^{III}(P)(X)(NO) + NO_3^- \tag{15}$$

A different reaction pathway was suggested recently to account for the formation of iron(II) nitrosyl species form nitrite complexes of iron(III) porphyrins [77]. According to this pathway, the oxygen transfer reaction involves the formation of a mixed oxidation state bridged intermediate (as shown in Scheme 10) and can only occur when both iron oxidation states are present in solution.

Despite the apparent instability of (porphinato)iron(III) nitrite derivatives in solution, such species have been synthesised and characterised [73,76,78].

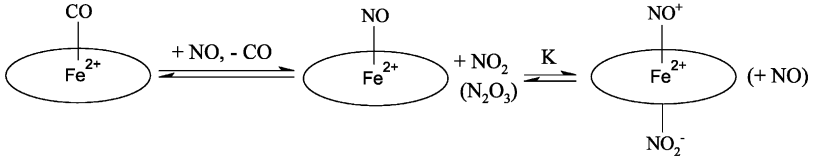

Scheme 9.

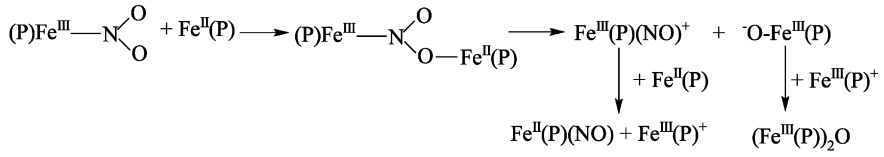

Scheme 10.

Similarly, the synthesis and structural features of five-coordinate $Fe^{II}(P)(NO_2^-)$ complexes have been reported in the literature [74,75]. The electronic features of nitrite complexes of ferric and ferrous porphyrins indicate that NO_2^- is *N*-bonded and acts as a strong π-acceptor ligand [73–75,78].

Very little kinetic and mechanistic information can be found on nitrite binding to model ferric and ferrous porphyrins, especially in aqueous media. Relatively more information is available on the kinetics of NO_2^- interaction with selected haemoproteins, such as haemoglobin, myoglobin and cytochrome *c* [79–81]. Although it may be concluded on the basis of these data that the reactions of synthetic and naturally occurring iron(II) and iron(III) porphyrins with nitrite are in general much slower than the respective reactions with NO, they do not allow us to comment on the details of the underlying reaction mechanisms. The interesting question is, however, what factors may account for the differences observed in the reaction kinetics exhibited by the two nucleophiles, viz. NO and NO_2^-.

In this context, a mechanistic study on the binding of nitrite to the ferrihaem centre in metmyoglobin has been carried out [82]. The reaction involves the binding of nitrite ion to the ferrihaem centre according to reaction (16).

$$\mathrm{metMb(H_2O) + NO_2^- \underset{k_{off}}{\overset{k_{on}}{\rightleftarrows}} metMb(NO_2^-) + H_2O} \qquad (16)$$

The rate of NO_2^- coordination to metMb(H_2O) was measured by stopped-flow technique as a function of [NO_2^-] at different temperatures and pressures. A comparison of the rate constants and activation parameters with those for the reaction of metMb(H_2O) with NO is presented in Table 8. Inspection of these data and the volume profiles for the reaction of metMb(H_2O) with NO and nitrite presented in Figs. 4a and 7, respectively, allows some interesting conclusions to be drawn:

(i) activation parameters obtained for the reaction of metMb with NO and NO_2^- clearly indicate that despite a significant difference in the 'on' reaction rates observed for the two nucleophiles, they react according to the same limiting dissociative mechanism, as controlled by the ferrihaem centre;

(ii) the observed volume of activation for the binding of nitrite to metMb is significantly smaller than that obtained for the reaction with NO. Obviously, structural changes on the protein accompanying the formation of the five-coordinate intermediate in the fast reaction with NO do not contribute to the volume change observed in the rate-determining step of the much slower reaction with nitrite;

(iii) the rate constants for the binding of nitrite to metMb(H_2O) are much smaller than those reported for the binding of NO, such that nitrite impurities will not interfere in studies on the interaction of metMb(H_2O) with NO.

Additional information on the observed differences in the 'on' reaction rates for nitrite and NO were obtained from DFT calculations performed for model Fe^{II}/Fe^{III} complexes with NO and NO_2^- as ligands [82]. The calculated energies indicate that the NO_2^- orbitals are higher in energy than those of NO, and this may

Table 8
Comparison of kinetic data for the reversible binding of NO_2^- and NO to metmyoglobin

Kinetic parameter	Forward reaction		Back reaction	
	metMb + NO_2^-	metMb + NO	metMb + NO_2^-	metMb + NO
Rate constant [a]	156 $M^{-1}\,s^{-1}$	2.7×10^4 $M^{-1}\,s^{-1}$	2.6 s^{-1}	16.0 s^{-1}
$\Delta H^{\ddagger}$ (kJ mol^{-1})	63 ± 1	71 ± 2	109 ± 2	78 ± 2
$\Delta S^{\ddagger}$ (J K^{-1} mol^{-1})	$+12\pm3$	$+82\pm7$	$+134\pm5$	$+46\pm7$
$\Delta V^{\ddagger}$ (cm^3 mol^{-1})	$+12\pm1$	$+21\pm1$	$+11.0\pm0.3$	$+16\pm1$

[a] Data measured at 20 °C (from Ref. [82]).

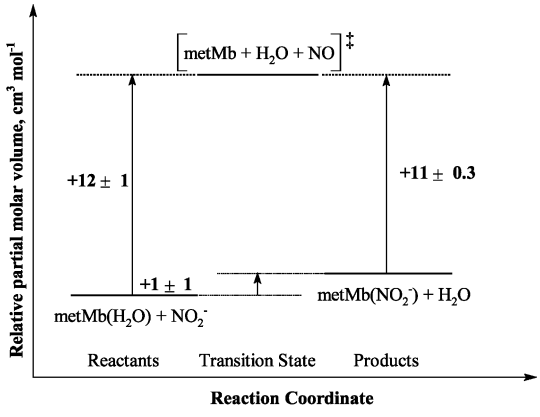

Fig. 7. Volume profile for the reversible binding of nitrite to metmyoglobin.

Zero-order path **First-order path**

$$NO_2^- + H^+ \rightleftharpoons HONO, \quad K_a$$

$$2\,HONO \xrightarrow{k_a} NO^+ + H_2O + NO_2^- \qquad Fe^{II}(edta) + HONO \xrightarrow{k_b} Fe^{III}(edta) + NO + OH^-$$

$$Fe^{II}(edta) + NO^+ \xrightarrow{fast} Fe^{III}(edta) + NO \qquad Fe^{II}(edta) + NO \xrightarrow{fast} Fe^{II}(edta)NO$$

$$Fe^{II}(edta) + NO \xrightarrow{fast} Fe^{II}(edta)NO$$

Scheme 11.

account for the fact that NO binds to metMb(H_2O) much faster than NO_2^-. As mentioned in the previous sections, NO binding to ferric porphyrins results in a partial charge transfer and the formal formation of Fe^{II}–NO^+. Calculations performed for NO^+ and model Fe(II) complexes show that ionisation of NO causes a significant decrease in its orbital energies and, as a consequence, a much better energy fit between the reacting molecules (i.e. NO^+ and Fe(II)). The calculations revealed that although NO binding to metMb(H_2O) is more favourable than that of NO_2^-, the resulting Fe^{III}–NO (or formally Fe^{II}–NO^+) bond is weaker than the Fe^{III}–NO_2^- bond. This result is in line with experimental findings that indicate larger k_{off} values for release of NO from metMb(NO) than the corresponding k_{off} values for dissociation of NO_2^-.

Interaction of Fe^{II}(edta) with NO_2^-/HONO can serve as an illustration of redox processes that may occur between a transition metal complex and nitrite present in the reaction medium. Apart from the fast reaction with NO (see Section 3), the Fe^{II}(edta) complex was observed to react with nitrite also [71]. This reaction occurs on a much slower time scale and leads to the formation of Fe^{II}(edta)NO and Fe^{III}(edta) as the final products, as shown in reaction (17).

$$2Fe^{II}(edta) + NO_2^- + 2H^+ \rightarrow Fe^{III}(edta) + Fe^{II}(edta)NO + H_2O \quad (17)$$

Detailed kinetic studies on the Fe^{II}(edta)/NO_2^-/HONO system revealed that the process observed occurs along two different reaction routes (viz. pseudo-first and pseudo-zero order in Fe^{II}(edta) content). The mechanism which accounts for the mixed order dependence and the observed reaction products consists of the reactions presented in Scheme 11 for the zero- and first-order paths, respectively.

The contribution of the different reaction paths and, in particular, the observed reaction rates strongly depend on pH and the total nitrite concentration, and can be accounted for in terms of the overall rate equation given in reaction (18).

$$-d[Fe(edta)]/dt = 2k_a[HONO]^2 + 2k_b[Fe(edta)][HONO] \quad (18)$$

The values of $k_a = 31\ M^{-1}\,s^{-1}$ and $k_b = 45\ M^{-1}\,s^{-1}$ were obtained from the experimental data [71]. A similar reactivity pattern has been observed in the reaction of nitrite with the reduced form of cobalamin (Cbl(II)), which has been shown to effectively bind NO on a microsecond time scale (see Section 4.3) [54]. Kinetic studies performed in order to compare the reactivity of reduced cobalamin towards NO and NO_2^-, have shown that nitrite can partially oxidise Cbl(II) to Cbl(III) and simultaneously produce NO, which rapidly binds to a second Cbl(II) molecule to form Cbl(III)(NO^-), in a process similar to that outlined for Fe^{II}(edta) complex. In the presence of excess nitrite, Cbl(II) can be converted to a mixture of Cbl(III)(NO_2^-) and Cbl(III)(NO^-), for which the overall reaction is given in (19).

$$2Cbl(II) + 2NO_2^- + 2H^+ \rightarrow Cbl(III)(NO_2^-) + Cbl(III)(NO^-) + H_2O \quad (19)$$

As in the case of the Fe^{II}(edta) complex, the observed reaction rate strongly increases with decreasing pH and increasing nitrite concentration, which can be accounted for in terms of an increase in [HONO]. However, only the pseudo-zero order reaction path, involving the formation of NO^+ from two molecules of HONO and its subsequent reaction with Cbl(II) (as depicted in Scheme 12) was observed.

Apparently, the pseudo-first order pathway does not contribute to the process observed under the selected experimental conditions, and the rate equation describing the reaction kinetics reduces to (20).

$$-d[Cbl(II)]/dt = 2k_a[HONO]^2 \quad (20)$$

The rate constant for the formation of NO^+ from nitrous acid determined in this system, $k_a = 18\ M^{-1}\,s^{-1}$, is in reasonable agreement with that obtained in the Fe^{II}(edta) study and with the corresponding values reported in literature [71].

Values of the pseudo-zero and pseudo-first order rate constants observed in the reactions of Fe^{II}(edta) and

$$2\,HONO \xrightarrow{k_a} NO^+ + H_2O + NO_2^-$$

$$Cbl(II) + NO^+ \xrightarrow{fast} Cbl(III) + NO$$

$$Cbl(II) + NO \xrightarrow{fast} Cbl(III)(NO^-)$$

Scheme 12.

Table 9
Values of pseudo-zero- and pseudo-first-order rate constants for the reaction of Fe^{II}(edta) and Cbl(II) with HONO and NO as a function of pH

pH	Fe(edta)+HONO $2k_a[HONO]^2$ ($M\,s^{-1}$) [a]	$2k_b[HONO]$ (s^{-1}) [a]	Cbl(II)+HONO $2k_a[HONO]^2$ ($M\,s^{-1}$) [b]
6.1	$<10^{-7}$	4.4×10^{-4}	$<10^{-7}$
5.1	4.7×10^{-7}	3.5×10^{-3}	1.1×10^{-6}
4.2	4.3×10^{-5}	5.9×10^{-2}	5.4×10^{-5}
3.4	7.5×10^{-4}	4.3×10^{-1}	8.3×10^{-4}
pH	Fe(edta)+NO k_{on}		Cbl(II)+NO [c] k_{on}
5.0	2.4×10^{8} $M^{-1}\,s^{-1}$ [d]		6.4×10^{8} $M^{-1}\,s^{-1}$
3.6	$\approx1\times10^{8}$ $M^{-1}\,s^{-1}$ [e]		5.3×10^{8} $M^{-1}\,s^{-1}$

[a] $[NO_2^-]_{total}=0.01$ M, 25 °C (Ref. [71]).
[b] Values calculated for $[NO_2^-]_{total}=0.01$ M from k_a determined experimentally at pH 4 (Ref. [54]).
[c] Data from Ref. [54].
[d] Data from Ref. [24].
[e] Data from Ref. [83].

Cbl(II) with HONO under the selected experimental conditions, are presented in Table 9. For comparison, the second-order rate constants for the binding of NO to these complexes at two selected pH values are also included. As can be seen from these data, oxidation of Fe^{II}(edta) and Cbl(II) by HONO is very slow at pH $\geq$ 5 for both systems, and will therefore not interfere in the studies on the reactions of these complexes with NO at higher pH. This reaction is, however, strongly accelerated by acid and may occur within seconds or minutes in sufficiently acidic solutions and/or at high nitrite concentration. Although the reaction rates observed in acidic solutions are still much smaller than those obtained for the binding of NO to Fe^{II}(edta) and Cbl(II), contamination of the samples with nitrite may, under certain conditions, lead to experimental difficulties is studying the reactions of such metal complexes with NO.

6. Conclusions

It was our aim with this review to focus on the question 'To be or not to be NO in coordination chemistry?' from a mechanistic point of view. The reported systems clearly show a number of general trends. The rate and mechanism of reactions of complexes of the type $M(L)H_2O$ with NO are in many cases controlled by the water exchange reaction on the metal centre. Complexes of the type $M^{n+}(L)NO$ are usually stabilised in solution by electron transfer to produce $M^{(n+1)+}(L)(NO^-)$ or $M^{(n-1)+}(L)(NO^+)$. NO behaves as a normal nucleophile in ligand substitution reactions to produce the nitrosylated products even though it is a radical. Finally, higher nitrogen oxides and NO_2^-/HONO can interfere with reactions of NO in aqueous solution and, in general, cause oxidation of $M(L)H_2O$. We thoroughly believe that further mechanistic investigations on the interaction of NO with other metal complexes and bio-relevant systems will contribute to an understanding of the biological behaviour and functions of this important molecule in even more complex systems.

Acknowledgements

The authors gratefully acknowledge the financial support from the Deutsche Forschungsgemeinschaft, Fonds der Chemischen Industrie, Max-Buchner-Forschungsstiftung, Akzo Nobel Functional Chemicals and Paques Bio Systems. The participation of Alicja Wanat, Thorsten Schneppensieper and Achim Zahl in many of the reported studies from this laboratory is highly appreciated.

References

[1] M. Hoshino, L. Laverman, P. Ford, Coord. Chem. Rev. 187 (1999) 75 (and references therein).
[2] W.R. Scheidt, M.K. Ellison, Acc. Chem. Res. 32 (1999) 350 (and references therein).
[3] A.L. Feig, M.T. Bautista, S.J. Lippard, Inorg. Chem. 35 (1996) 6892 (and references therein).
[4] J.A. Farrar, R. Grinter, D.L. Pountney, A.J. Thomson, J. Chem. Soc. Dalton Trans. (1993) 2703 (and references therein).
[5] Y. Henry, A. Guissani, Cell. Mol. Life Sci. 55 (1999) 1003.
[6] J.A. McCleverty, Chem. Rev. 79 (1979) 53.
[7] J.H. Enemark, R.D. Feltham, Coord. Chem. Rev. 13 (1974) 339.
[8] W.R. Scheidt, H.F. Duval, T.J. Neal, M.K. Ellison, J. Am. Chem. Soc. 122 (2000) 4651.
[9] A. Ghosh, T. Wondimagegn, J. Am. Chem. Soc. 122 (2000) 8101.
[10] G.B. Richter-Addo, R.A. Wheeler, Ch.A. Hixson, L. Chen, M.A. Khan, M.K. Ellison, Ch.E. Schulz, W.R. Scheidt, J. Am. Chem. Soc. 123 (2001) 6314.
[11] R.G. Hayes, M.K. Ellison, W.R. Scheidt, Inorg. Chem. 39 (2000) 3665.
[12] (a) P.A. Duffin, L.F. Larkworthy, J. Mason, A.N. Stephens, R.M. Thompson, Inorg. Chem. 26 (1987) 2034;
(b) J. Bultitude, L.F. Larkworthy, J. Mason, D.C. Povey, B. Sandell, Inorg. Chem. 23 (1984) 3629;
(c) C.J. Groombridge, L.F. Larkworthy, J. Mason, Inorg. Chem. 32 (1993) 379.
[13] Y. Chen, F. Lin, R.E. Shepherd, Inorg. Chem. 38 (1999) 973.
[14] D.S. Bohle, Ch. Hung, B.D. Smith, Inorg. Chem. 37 (1998) 5798.
[15] M.K. Ellison, Ch.E. Schulz, W.R. Scheidt, Inorg. Chem. 39 (2000) 5102.
[16] Ch. Hauser, T. Glaser, B. Eckhard, T. Weyhermüller, K. Wieghardt, J. Am. Chem. Soc. 122 (2000) 4352 (and references therein).
[17] C.A. Brown, M.A. Pavlowsky, T.E. Westre, Y. Zhang, B. Hedman, K.O. Hodgson, E.I. Solomon, J. Am. Chem. Soc. 117 (1995) 715 (and references therein).
[18] J.H. Rodriguez, Y. Xia, P.G. Debrunner, J. Am. Chem. Soc. 121 (1999) 7846.

[19] R.E. Shepherd, M.A. Sweetland, D.E. Junker, J. Inorg. Biochem. 53 (1997) 1.
[20] M.S. Ward, R.E. Shepherd, Inorg. Chim. Acta 286 (1999) 197.
[21] Y. Chen, M.A. Sweetland, R.E. Shepherd, Inorg. Chim. Acta 260 (1997) 163.
[22] K.J. Franz, S.J. Lippard, J. Am. Chem. Soc. 121 (1999) 10504.
[23] T. Schneppensieper, S. Finkler, A. Czap, R. van Eldik, M. Heus, P. Nieuwenhuizen, C. Wreesmann, W. Abma, Eur. J. Inorg.Chem. (2001) 491.
[24] T. Schneppensieper, A. Wanat, G. Stochel, S. Goldstein, D. Meyerstein, R. van Eldik, Eur. J. Inorg. Chem. (2001) 2317 (and references therein).
[25] T. Schneppensieper, A. Wanat, A. Stochel, R. van Eldik, Inorg. Chem., in press.
[26] T. Mizuta, J. Wang, K. Miyoshi, Inorg. Chim. Acta 230 (1995) 119 (and references therein).
[27] A. Wanat, T. Schneppensieper, G. Stochel, R. van Eldik, B. Eckhard, K. Wieghardt, Inorg. Chem. 41 (2002) 4.
[28] Y. Ducommun, K.E. Newman, A.E. Merbach, Inorg. Chem. 19 (1980) 3696–3703.
[29] A.M. Rich, R.S. Armstrong, P.J. Ellis, P.A. Lay, J. Am. Chem. Soc. 120 (1998) 10827.
[30] J.F. Deatherage, K.J. Moffat, J. Mol. Biol. 134 (1979) 401.
[31] E. Obayaashi, K. Tsukamoto, S. Adachi, S. Takahashi, M. Nomura, T. Iizuka, H. Shoun, Y. Shiro, J. Am. Chem. Soc. 119 (1997) 7807.
[32] M. Hoshino, K. Ozawa, H. Seki, P.C. Ford, J. Am. Chem. Soc. 115 (1993) 9568.
[33] L.E. Laverman, A. Wanat, J. Oszajca, G. Stochel, P.C. Ford, R. van Eldik, J. Am. Chem. Soc. 123 (2001) 285.
[34] W.R. Scheidt, Y.J. Lee, K. Hatano, J. Am. Chem. Soc. 106 (1984) 3191.
[35] M. Hoshino, M. Maeda, R. Konishi, H. Seki, P.C. Ford, J. Am. Chem. Soc. 118 (1996) 5702.
[36] L.E. Laverman, M. Hoshino, P.C. Ford, J. Am. Chem. Soc. 119 (1997) 12663.
[37] L.E. Laverman, P.C. Ford, Chem. Commun. (1999) 1843.
[38] T. Yoshimura, S. Suzuki, Inorg. Chim. Acta 152 (1988) 241–249 (and references therein).
[39] T. Schneppensieper, A. Zahl, R. van Eldik, Angew. Chem. Int. Ed. Engl. 40 (2001) 1678.
[40] D.S. Bohle, P. Debrunner, J.P. Fitzgerald, B. Hansert, Ch. Hung, A.J. Thomson, Chem. Commun. (1997) 91.
[41] D.S. Bohle, Ch. Hung, J. Am. Chem. Soc. 117 (1995) 9584.
[42] (a) L.S. Miller, A.J. Pedraza, M.R. Chance, Biochemistry 36 (1997) 12199;
(b) Y. Wang, B.A. Averill, J. Am. Chem. Soc. 118 (1996) 3972.
[43] A. Drljaca, C.D. Hubbard, R. van Eldik, T. Asano, M.V. Basilewsky, W.J. le Noble, Chem. Rev. 98 (1998) 2167.
[44] L. Helm, A.E. Merbach, J. Coord. Chem. 187 (1999) 151.
[45] M.D. Wirt, I. Sagi, E. Chen, S.M. Frisbie, R. Lee, M.R. Chance, J. Am. Chem. Soc. 113 (1991) 5299.
[46] B. Krautler, W. Keller, C. Kratky, J. Am. Chem. Soc. 111 (1989) 8936.
[47] C. Rovira, K. Kunc, J. Hutter, M. Parrinello, Inorg. Chem. 40 (2001) 11.
[48] K.L. Brown, X. Zou, M. Marques, J. Mol. Struct. (THEOCHEM) 453 (1998) 209.
[49] S.S. Greenberg, J.X. Xie, J.M. Zatarain, D.R. Kapusta, M.J. Miller, J. Pharmacol. Exp. Ther. 273 (1995) 257.
[50] M. Brouwer, W. Chamulitrat, G. Ferruzzi, D.L. Saulus, J.B. Weinberg, Blood 88 (1996) 1857.
[51] H. Kruszyna, J.S. Magyar, L.G. Rochelle, M.A. Russel, R.P. Smith, D.E. Wilcox, J. Pharmacol. Exp. Ther. 285 (1998) 665 (and references therein).
[52] D. Zheng, R. Birke, J. Am. Chem. Soc. 123 (2001) 4637 (and references therein).
[53] M. Wolak, G. Stochel, M. Hamza, R. van Eldik, Inorg. Chem. 39 (2000) 2018 (and references therein).
[54] M. Wolak, A. Zahl, T. Schneppensieper, R. van Eldik, J. Am. Chem. Soc. 123 (2001) 9780.
[55] K.A. Connors, Chemical Kinetics, VCH, New York, 1990, p. 135.
[56] R. van Eldik, H. Cohen, D. Meyerstein, Inorg. Chem. 33 (1994) 1566.
[57] (a) G.N. Schrauzer, L. Lee, J. Am. Chem. Soc. 90 (1964) 6541;
(b) I. Sagi, M.D. Wirt, S. Frisbie, M.R. Chance, J. Am. Chem. Soc. 112 (1990) 8641;
(c) M. Giorgetti, I. Ascone, M. Berrettoni, P. Conti, S. Zamponni, R.J. Marassi, Biol. Inorg. Chem. 5 (2000) 156.
[58] M. Feelish, J.S. Stamler (Eds.), Methods in Nitric Oxide Research, Wiley, Chichester, UK, 1996, p. 8.
[59] I.M. Lorković, P.C. Ford, Inorg. Chem. 39 (2000) 632.
[60] R. Lin, P.J. Farmer, J. Am. Chem. Soc. 123 (2001) 1143.
[61] I.M. Lorković, K.M. Miranda, B. Lee, S. Bernhard, J.R. Schoonover, P.C. Ford, J. Am. Chem. Soc. 120 (1998) 11647.
[62] I.M. Lorković, P.C. Ford, Inorg. Chem. 38 (1999) 1467.
[63] S.K. O'Shea, W. Wang, R.S. Wade, C.E. Castro, J. Org. Chem. 61 (1996) 6388.
[64] O.Q. Munro, W.R. Scheidt, Inorg. Chem. 37 (1998) 2308.
[65] M. Feelish, J.S. Stamler (Eds.), Methods in Nitric Oxide Research, Wiley, Chichester, UK, 1996, p. 128.
[66] G. Stochel, R. van Eldik, E. Hejmo, Z. Stasicka, Inorg. Chem. 27 (1988) 2767.
[67] A.A. Chevalier, L.A. Gentil, V.T. Amorebieta, M.M. Gutiérrez, J.A. Olabe, J. Am. Chem. Soc. 122 (2000) 11238.
[68] B.A. Averill, Chem. Rev. 96 (1996) 2951.
[69] I. Maciejowska, Z. Stasicka, G. Stochel, R. van Eldik, J. Chem. Soc. Dalton Trans. (1999) 3643.
[70] M.R. Rhodes, M.H. Barley, T. Meyer, J. Inorg. Chem. 30 (1991) 629.
[71] V. Zang, M. Kotowski, R. van Eldik, Inorg. Chem. 27 (1988) 3279 (and references therein).
[72] M.G. Finnegan, A.G. Lappin, W.R. Scheidt, Inorg. Chem. 29 (1990) 181 (and references therein).
[73] H. Nasri, Y. Wang, B.H. Huynh, F.A. Walker, W.R. Scheidt, Inorg. Chem. 30 (1991) 1483.
[74] H. Nasri, Y. Wang, B.H. Huynh, W.R. Scheidt, J. Am. Chem. Soc. 113 (1991) 717.
[75] H. Nasri, M.K. Ellison, S. Chen, B.H. Huynh, W.R. Scheidt, J. Am. Chem. Soc. 119 (1997) 6274.
[76] M.K. Ellison, Ch.E. Schulz, W.R. Scheidt, Inorg. Chem. 38 (1999) 100.
[77] Z. Wie, M.D. Ryan, Inorg. Chim. Acta 314 (2001) 49 (and references therein).
[78] H. Nasri, A. Goodwin, W.R. Scheidt, Inorg. Chem. 29 (1990) 185.
[79] M. Antonini E. Brunori, Hemoglobin and Myoglobin in Their Reactions with Ligands, North-Holland, Amsterdam, 1971 (and references therein).
[80] (a) J. Blanck, W. Graf, W. Scheler, Acta Biol. Med. Ger. 7 (1961) 323;
(b) W. Graf, J. Blanck, W. Scheler, Acta Biol. Med. Ger. 9 (1962) 1;
(c) J. Blanck, W. Scheler, Acta Biol. Med. Ger. 20 (1968) 721.
[81] J. Mintorovitch, J.D. Satterlee, Biochemistry 27 (1988) 8045.
[82] A. Wanat, J. Gdula-Argasinska, D. Rutkowska-Zbik, M. Witko, G. Stochel, R. van Eldik, J. Biol. Inorg. Chem. 7 (2002) 165.
[83] W. Weisweiler, R. Blumhofer, T. Westermann, Chem. Eng. Proc. 20 (1986) 155.